

Metal Complexes

Interaction between Anions and Cationic Metal Complexes Containing Tridentate Ligands with *exo*-C–H Groups: Complex Stability and Hydrogen BondingHéctor Martínez-García,^[a] Dolores Morales,^[a, b] Julio Pérez,^{*[a]} Marcos Puerto,^[a] and Ignacio del Río^[a]

Abstract: $[\text{Re}(\text{CO})_3([\text{9}]\text{aneS}_3)][\text{BAR}'_4]$ (**1**), prepared by reaction of $\text{ReBr}(\text{CO})_5$, 1,4,7-trithiacyclononane ($[\text{9}]\text{aneS}_3$) and NaBAR'_4 , forms stable, soluble supramolecular adducts with chloride (**2**), bromide, methanesulfonate (**3**) and fluoride (**4**) anions. These new species were characterized by IR, NMR spectroscopy and, for **2** and **3**, also by X-ray diffraction. The results of the solid state structure determinations indicate the formation of $\text{CH}\cdots\text{X}$ hydrogen bonds between the anion (X) and the *exo*-C–H groups of the $[\text{9}]\text{aneS}_3$ ligand, in accord with the relatively large shifts found by ^1H NMR spectroscopy in dichloromethane solution for those hydrogens. The stability of the chloride adduct contrasts with the lability of the $[\text{9}]\text{aneS}_3$ ligand in allyldicarbonyl molybdenum complexes recently studied by us. With fluoride, in dichloromethane solution, a second, minor neutral dimeric species **5** is formed in addition to **4**. In **4**, the deprotonation of a C–H group of the $[\text{9}]\text{aneS}_3$ ligand, accompanied by C–S bond cleavage and dimerization, afforded **5**, featuring bridging thiolates. Compounds $[\text{Mo}(\eta^3\text{-methallyl})(\text{CO})_2(\text{TpyN})][\text{BAR}'_4]$ (**6**) and $[\text{Mo}(\eta^3\text{-methallyl})(\text{CO})_2(\text{TpyCH})][\text{BAR}'_4]$ (**7**) were synthesized by the reactions of $[\text{MoCl}(\eta^3\text{-methallyl})(\text{CO})_2(\text{NCMe})_2]$, NaBAR'_4 and tris(2-pyridyl)amine (TpyN) or tris(2-pyridyl)methane (TpyCH) respectively, and characterized by IR and ^1H and ^{13}C NMR spectroscopy in solution, and by X-ray diffraction in the solid state. Compound **6** undergoes facile substitution of one of the 2-pyridyl groups by chloride, bromide, and methanesulfonate anions. Stable supramolecular adducts were formed between **7** and chloride, bromide, iodide, nitrate, and perchlorate anions. The solid state structures of these adducts (**12–16**) were determined by X-ray diffraction. Binding constants in dichloromethane were calculated from ^1H NMR titration data for all the new supramolecular adducts. The signal of the bridgehead C–H group is the one that undergoes a more pronounced downfield shift when tetrabutylammonium chloride was added to **7**, whereas smaller shifts were found for the 2-pyridyl C(3)–H groups. In agreement, both types of C–H groups form hydrogen bonds to the anions in the solid state structures.

Introduction

Most synthetic anion receptors employ several hydrogen bond donor groups placed in appropriate positions for anion binding, often in combination with the electrostatic attraction resulting from a positive charge in the host.^[1] This is also true of one type of metal-based host, in which the metal, rather than directly binding the anions, pre-organizes the set of ligands and restricts their degrees of freedom, orienting their hydrogen bond donor groups in a convergent geometry, able to act

cooperatively toward the anionic guest.^[2] In most of these hosts, the hydrogen bond donor groups are N–H groups of functions such as ammonium groups, amides, pyrroles, etc. In some cases, appropriately placed C–H groups can cooperate with the N–H groups.^[3] Few hosts employ C–H groups as the only hydrogen bond donor groups and, among them, the Pd-based receptor reported by Bedford, Tucker, and coworkers has been the first that uses only aliphatic C–H groups as hydrogen-bond donors.^[4] In this receptor, coordination to the Pd^{II} center rigidifies the ligand 1,4,7-trithiacyclononane ($[\text{9}]\text{aneS}_3$) in such a conformation that its *exo*-C–H groups converge towards an external anion. A weakness of this host, as with many other metal-based hosts, is its lack of stability towards the most nucleophilic anions. Thus, the Pd-based host undergo displacement of the $[\text{9}]\text{aneS}_3$ ligand in presence of chloride or bromide. The cyclic thioether $[\text{9}]\text{aneS}_3$ is, in general, a very good ligand when it forms metal complexes acting as a fac-capping tridentate ligand, because, in the most stable conformation of the free ligand, the three sulfur atoms are disposed in optimal orientations for metal complexation. As such, little reorganization of the ligand is required for complex forma-

[a] Dr. H. Martínez-García, Dr. D. Morales, Dr. J. Pérez, Dr. M. Puerto, Dr. I. del Río
Departamento de Química Orgánica e Inorgánica- CINN
Facultad de Química, Universidad de Oviedo-CSIC
33006 Oviedo (Spain)
Fax: (+34) 985103446
E-mail: japm@uniiovi.es

[b] Dr. D. Morales
Instituto Tecnológico de Materiales (ITMA). Parque Tecnológico de Asturias,
33428 Llanera (Asturias)

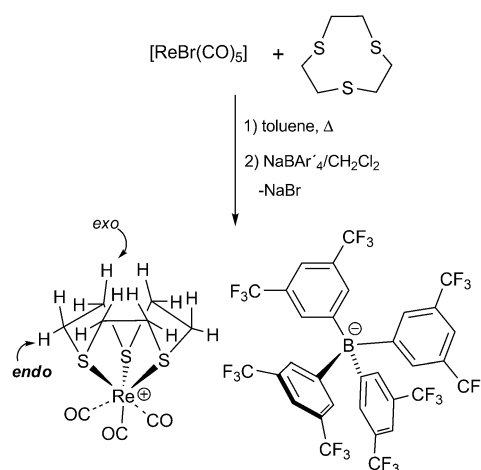
Supporting information for this article is available on the WWW under <http://dx.doi.org/10.1002/chem.201303653>.

tion.^[5] Inspired by the work of Bedford, Tucker, and coworkers, we hypothesized that a metal fragment with a preference for a pseudooctahedral geometry would form more stable complexes with [9]aneS₃ than the Pd^{II} center used by those authors. Therefore, we synthesized and characterized complexes of [9]aneS₃ with the pseudooctahedral fragments Mo(methallyl)(CO)₂ and Mo(allyl)(CO)₂, and studied their behavior in dichloromethane solution in the presence of several anions.^[6] The results demonstrated that the molybdenum complexes were more stable than the Pd-based hosts, because the former were stable in the presence of bromide; in fact, the solid-state structure of the hydrogen bonded bromide-host ion pair could be determined by X-ray diffraction. However, the more nucleophilic chloride anion completely and rapidly displaced the [9]aneS₃ ligand in dichloromethane solution at room temperature to form the known chloride-bridged binuclear anionic [Mo(η³-methallyl)(CO)₂]₂(μ-Cl)₃⁻ complexes. In view of these results, we endeavored to synthesize more stable, cationic metal complexes of [9]aneS₃ and study their behavior toward anions, including chloride. We have followed two different approaches aiming to obtain hosts more stable than our previously reported molybdenum complexes of [9]aneS₃: first, we prepared a complex of [9]aneS₃ with the Re(CO)₃ fragment. In comparisons between the two series of complexes, we have previously found that rhenium tricarbonyl complexes are more stable toward substitution of neutral ligands by anions than Mo(allyl)(CO)₂ complexes.^[7] Moreover, the compound [Re(CO)₃([9]aneS₃)]Br was previously known, and its identity has been conclusively demonstrated by X-ray diffraction.^[8] Second, since we have previously found that 2,2'-bipyridine, a bis(2-pyridyl) ligand, forms with the Mo(methallyl)(CO)₂ fragment, complexes which are very stable in the presence of anions, including chloride,^[3b] we have employed that same metal fragment in combination with the *fac*-capping tris(2-pyridyl)amine (TpyN) and tris(2-pyridyl)methane (TpyCH) ligands,^[9] under the hypothesis that the C–H groups at the backside of the coordinated ligands would provide good hydrogen bond donor groups toward external anions. The interaction between the C–H groups of metal-coordinated pyridines and anions has been studied by Gale et al.^[2h] Very recently, Sanford et al. reported hydrogen bonding between chloride and other counteranions and the pyridyl C–H groups of a Pd^{IV}-coordinated TpyCH ligand of the same type that will be discussed below.^[10] Constable et al. have demonstrated, both in solution and the solid state, a significant interaction between chloride and the 3,3'-CH groups of a coordinated 2,2'-bipyridine ligand in an Ir^{III} complex.^[11] A similar interaction has been found for Ru^{II} complexes by Meyer et al.^[12] In both approaches we have prepared the cationic complexes as salts of the BAR'₄ (Ar' = 3,5-bis(trifluoromethyl)phenyl),^[13] because this anion has a very low tendency to act as hydrogen bond acceptor^[14] and, therefore, should compete less than other counteranions with external anions for hydrogen bonding the cationic host. Our results are described in what follows.

Results

Rhenium trithiacyclononane compounds

The reaction of equimolar amounts of ReBr(CO)₅, [9]aneS₃, and NaBAR'₄ in refluxing toluene afforded the new compound [Re(CO)₃([9]aneS₃)] [BAR'₄] (1) as the single product in 85 % yield as a white microcrystalline powder (Scheme 1). As is typical of



Scheme 1. Synthesis of 1.

BAR'₄ salts, 1 was found to be very soluble in dichloromethane and non-aqueous oxygenated solvents such as tetrahydrofuran, acetone, and diethylether. Its IR νCO bands (2058 and 1974 cm⁻¹ in CH₂Cl₂) are consistent with the presence of a cationic *fac*-tricarbonyl complex.^[15] The ¹H NMR spectrum of 1 features two multiplets for the CH₂ groups of the [9]aneS₃ ligand (at 3.05 and 2.74 ppm in CD₂Cl₂, one for the *endo* and other for the *exo* hydrogens), indicating that the trithioether ligand does not dissociate (the ¹H NMR of free [9]aneS₃ consists of one singlet), and the C₃ symmetry of the complex. The three-fold symmetry of the complex (which, in turn, indicates tridentate coordination of the [9]aneS₃ ligand) was confirmed by the presence of single signals for the CO (186.4 ppm) and [9]aneS₃ (34.5 ppm) ligands in the ¹³C NMR spectrum of 1.

The behavior of 1 towards the tetrabutylammonium salts of fluoride, chloride, bromide, iodide, hydrogensulfate, and methanesulfonate in dichloromethane were studied by IR and ¹H NMR spectroscopies. The unique behavior of fluoride will be discussed below. The addition of tetrabutylammonium chloride shifted the IR νCO bands of 1 only marginally to lower frequencies, indicating hydrogen bonding, rather than formation of a direct Re–Cl bond by a substitution reaction, in contrast with the results found for the molybdenum complexes.^[6] The successive additions of [Bu₄N]Cl shifted the ¹H NMR multiplet initially at 2.74 ppm to higher frequencies, whereas the signal at 3.05 ppm remained virtually unchanged. This demonstrates that the signal at 2.74 ppm in 1 corresponds to the *exo* hydrogens, pointing outward from the metal and, therefore, more accessible for the contact with the anions (See Scheme 1). The response of the ¹H NMR chemical shift to the addition of hy-

drogen-bond acceptors has been used to differentiate between hydrogens with different accessibility in polyamine complexes.^[16] Along the series of these additions of [Bu₄N]Cl, only one set of signals were observed in the ¹H NMR spectra, indicating fast anion exchange. After addition of one equivalent of [Bu₄N]Cl, the magnitude of the shift spanned more than one ppm. The variation of the chemical shift in response to the addition of chloride was used to generate a Job plot, shown in the Supporting Information, which indicated the formation of an adduct of 1:1 stoichiometry. A plot of the variation of the chemical shift against the amount of chloride added is shown in Figure 1. Treatment of these data with the WinEQNMR program^[17] provided a 10⁴ value for the binding constant (Table 1). This high value is in line with the saturation behavior indicated by the horizontal line reached after one equivalent of chloride was added.

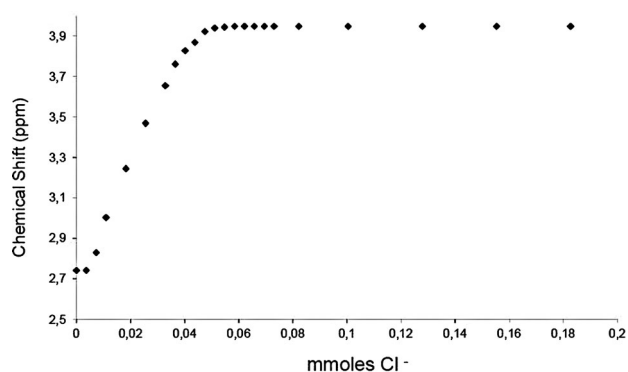


Figure 1. ¹H NMR titration profile of **1** with [Bu₄N]Cl in CD₂Cl₂.

A similar behavior has been found for bromide and methanesulfonate (see Table 1 and the Supporting Information), with slightly lower binding constants, as expected for larger anions. When tetrabutylammonium salts of iodide and hydrogensulfate were added to **1**, a large amount of a white precipitate, quite insoluble in most organic solvents, was formed. When tetraethylammonium iodide and [PPN]I were used in place of

[Bu₄N]I, analogous precipitations took place, indicating that the nature of the counteranion does not affect the insolubility of the species formed (PPN = bis(triphenylphosphoranylidene)ammonium). Therefore, no further studies were carried out with iodide and hydrogensulfate.

The synthesis and the solid state structural determination by single crystal X-ray diffraction of compound [Re(CO)₃([9]aneS₃)]Br has been reported by Wiegardt and coworkers.^[8] The results demonstrate that the cation present in **1** is stable towards displacement of the [9]aneS₃ ligand by bromide.

Equimolar amounts of **1** and tetrabutylammonium chloride were combined in dichloromethane. After solvent evaporation and washing the solid residue with diethylether to remove [Bu₄N][BAR'₄], the compound [Re(CO)₃([9]aneS₃)]Cl (**2**) was crystallized from dichloromethane/hexane. Its structure was determined by X-ray diffraction, and a thermal ellipsoid plot is shown in Figure 2. Compound **2** consists of a C_{3v}-symmetric [Re(CO)₃([9]aneS₃)]⁺ complex with the chloride anion sitting on top of the coordinated thioether and forming hydrogen bonds with three of the *exo* C–H groups. The relatively short C...Cl distances, 3.551(0) angströms, and large C...H...Cl angles of 167.9(0) degrees, are consistent with significant C–H...Cl hydrogen bonds, in agreement with the relatively large (for an aliphatic C–H group) downfield shift of the ¹H NMR signals of the C–H groups upon chloride addition described above.

Attempts to crystallize the methanesulfonate adduct by a procedure analogous to that given above for **2** afforded the hydrate [Re(CO)₃([9]aneS₃)](SO₃Me)·H₂O (**3**). Its structure, determined by X-ray diffraction, is shown in Figure 3. The three oxygen atoms of the anion act as hydrogen-bond acceptors, two of them with C–H groups of the thioether ligand, and the third with the water molecule. Despite the multi-point hydrogen bonding of the methanesulfonate anion, its binding constant (Table 1) is lower than those with chloride and bromide, as expected for an oxoanion, larger and with more charge delocalization over the highly electronegative oxygen atoms. Moreover, the fact that one of the oxygen atoms forms exclusively a hydrogen bond with the water molecule suggests that

Table 1. Stability constants of the cation complexes with various anions in the form of tetrabutylammonium salts; determined by ¹ H NMR titration in CD ₂ Cl ₂ . Δδ (ppm) max of the signal considered for K _a determination.								
Receptor		Cl ⁻	Br ⁻	I ⁻	CH ₃ SO ₃ ⁻	HSO ₄ ⁻	NO ₃ ⁻	ReO ₄ ⁻
1	K _a (M ⁻¹)	12729 ± 826	11440 ± 1572	–	7985 ± 1125	–	–	–
	Δδ (ppm)	1.20	1.11	–	0.82	–	–	–
	K _a (M ⁻¹)	515 ± 93 ^[a]	498 ± 25 ^[a]	54 ± 5 ^[a]	340 ± 29 ^[a]	–	89 ± 11 ^[a]	204 ± 15 ^[a]
		447 ± 100 ^[b]	533 ± 84 ^[b]	113 ± 8 ^[b]	324 ± 19 ^[b]	–	98 ± 13 ^[b]	185 ± 5 ^[b]
7	Δδ (ppm)	2.65 ^[c]	2.49 ^[c]	2.04 ^[c]	1.55 ^[c]	–	1.38 ^[c]	0.66 ^[d]
		1.09 ^[d]	1.06 ^[d]	1.02 ^[d]	0.80 ^[d]	–	0.63 ^[d]	0.37 ^[d]
[Mo(η ³ -methyllyl)([9]aneS ₃)(CO) ₂] ⁺ [e]	K _a (M ⁻¹)	–	2320 ± 139	4699 ± 257	2933 ± 202	3839 ± 685	–	–
	Δδ (ppm)	–	0.97	0.86	0.75	0.69	–	–
[Mo(η ³ -allyl)([9]aneS ₃)(CO) ₂] ⁺ [e]	K _a (M ⁻¹)	–	11252 ± 1503	14408 ± 2301	15990 ± 2514	–	–	–
	Δδ (ppm)	–	0.98	0.87	0.75	–	–	–

[a] Stability constants determined by following bridgehead CH resonance and [b] H3 (py) resonance [c] Δδ max determined from the titration curves following bridgehead CH and [d] H3 (py) resonance shift. [e] Related receptor complexes described in reference 6.

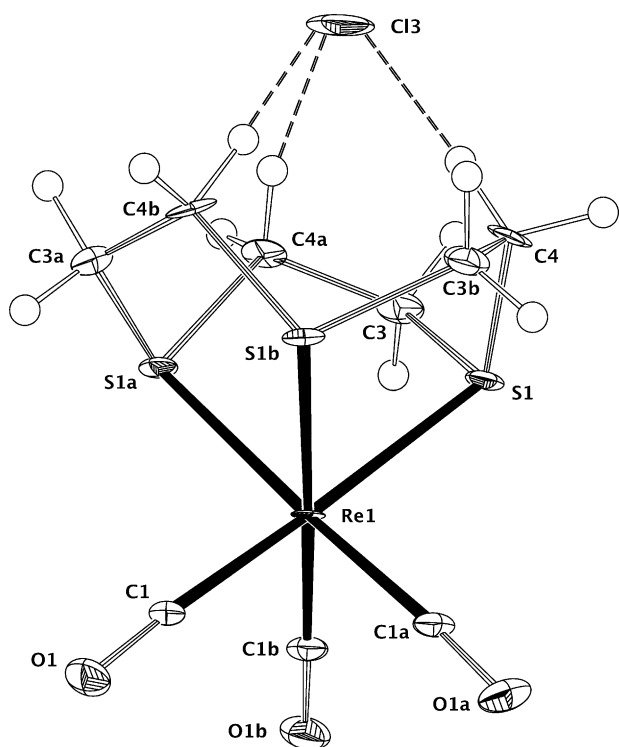


Figure 2. Thermal-ellipsoid (50%) plot of **2**. Main hydrogen bond distances (Å) and angles (°): C···Cl 3.551(0), C···H···Cl 167.9(0).

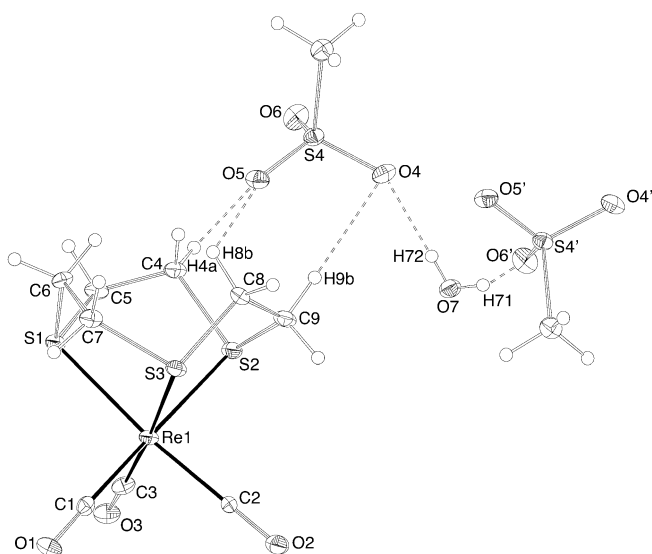


Figure 3. Thermal-ellipsoid (30%) plot of **3**. Main hydrogen bond distances (Å) and angles (°): C9–O4 3.564(0), C8–O5 3.405(0), C4–O5 3.307(0), O7–O4 2.843(0), O7–O6 2.906(0); C9–H9b–O4 169.53(0); C8–H8b–O5 151.84(0), C4–H4a–O5 124.10(0), O7–H72–O4 163.75(0), O7–H71–O6 170.87(0).

the presence of water, a better hydrogen bond donor than the C–H groups of the coordinated [9]aneS₃, can exert a significant screening of the interaction between the anion and the C–H groups.

When compound **1** was treated with an equimolar amount of tetrabutylammonium fluoride in dichloromethane, the IR

ν CO bands decreased slightly, in accordance with the formation of a hydrogen bonded ion pair [Re(CO)₃([9]aneS₃)]F (**4**), like in the case of chloride or bromide. The ¹H NMR spectrum of **4** in CD₂Cl₂ displays multiplets at 3.75 and 2.94 ppm, diagnostic of coordinated, non-labile [9]aneS₃. Compound **4** can be trapped by carrying out the reaction between **1** and tetrabutylammonium fluoride in diethylether, a good solvent for both reagents, but in which **4** is insoluble and precipitates as a white powder. However, in dichloromethane solution, a second, minor species **5** is formed in addition to **4**. Compound **5** displays IR ν CO bands at 2013 and 1917 cm⁻¹. Initially, these bands, much lower than those of **1**, made us suspect of a substitution of the thioether ligand by fluoride or by the hydroxide anion generated by water (the tetrabutylammonium fluoride is a trihydrate) deprotonated by fluoride (Scheme 2), because that was the case in the reaction of [Mo(η^3 -methallyl)(CO)₂([9]aneS₃)] [BAR'₄] with tetrabutylammonium fluoride.^[6] However, ¹H NMR spectra of the reaction crude did not show the presence of free [9]aneS₃. The product of the reaction of **1** with [Bu₄N]F·3H₂O was washed with Et₂O to remove the [Bu₄N][BAR'₄] byproduct. The residue was dissolved in CH₂Cl₂ and the resulting solution was layered with hexane and allowed to slowly diffuse. Despite repeated attempts, we have not been able to obtain X-ray quality crystals of **4**. A single crystal of **5** was employed for the determination of its solid-state structure. Despite the low quality of the results, they demonstrated that **5** is the neutral dimeric complex shown in Figure 4.

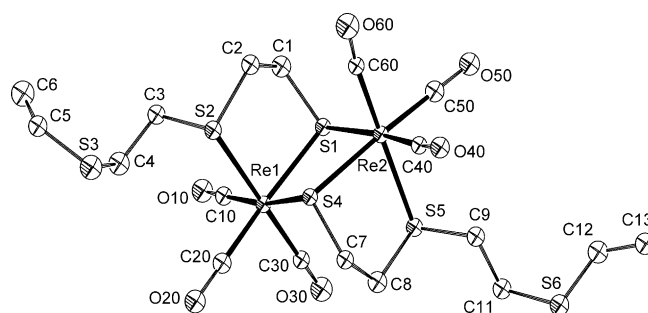
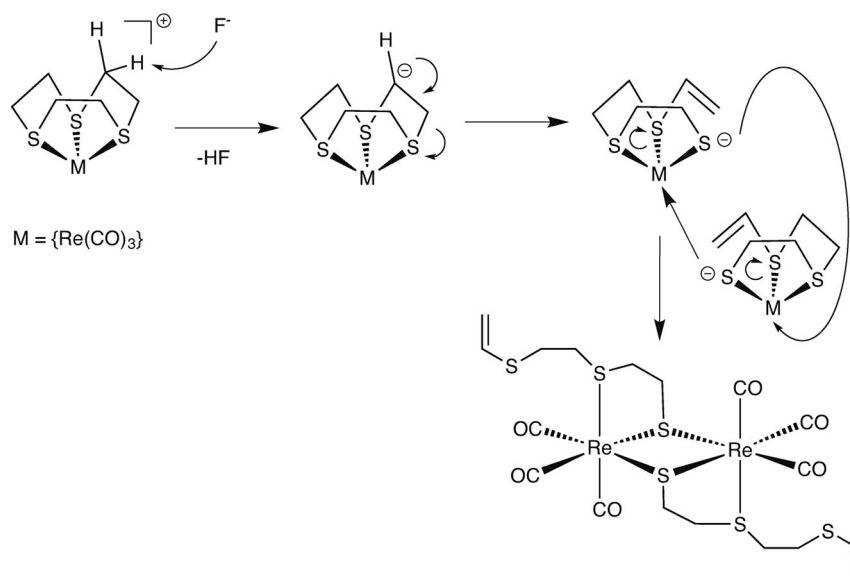


Figure 4. Thermal-ellipsoid (30%) plot of **5**.

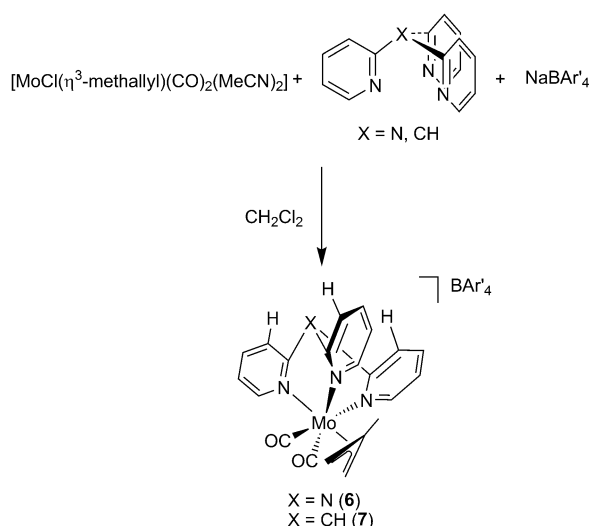
Molybdenum complexes of tris(2-pyridyl) ligands

Compounds [Mo(η^3 -methallyl)(CO)₂(TpyN)][BAR'₄] (**6**) and [Mo(η^3 -methallyl)(CO)₂(TpyCH)][BAR'₄] (**7**) were synthesized by the reactions of [MoCl(η^3 -methallyl)(CO)₂(NCMe)₂]^[18] NaBAR'₄^[13] and the ligands tris(2-pyridyl)amine (TpyN) or tris(2-pyridyl)methane (TpyCH), respectively^[9] (see Scheme 3), and characterized by IR and ¹H and ¹³C NMR spectroscopies in solution and by X-ray diffraction in the solid state.

The IR spectra of **6** and **7**, each containing two broad ν CO bands, indicate their *cis*-dicarbonyl geometry, and the fact that the more intense band is that at higher frequency indicates acute OC–Mo–CO angles.^[6] The relatively high wavenumber values of the IR ν CO bands is in agreement with the presence of cationic complexes. The ¹H NMR spectra confirm the pres-



Scheme 2. Proposed mechanism for the formation of 5.



Scheme 3. Synthesis of compounds 6 and 7.

ence of one BAR'_4 anion per molybdenum; that is, a BAR'_4 :methylalyl:tris(2-pyridyl) ligand ratio of 1:1:1. The presence of separate signals for the *syn* and *anti* methylalyl hydrogens indicates that the methylalyl group is coordinated in a static η^3 mode. Two signals in a 1:2 ratio are observed for the H6 hydrogens of the 2-pyridyl groups in the room temperature ^1H NMR spectra of compounds 6 and 7, reflecting the existence of a mirror plane in the cationic complexes, and their rigidity. The latter contrasts with the dynamic behavior of [9]aneS₃ derivatives, which leads to apparent C₃-symmetry at room temperature.^[6] The solid state structures of the cationic complexes, shown in Figures 5 (6) and 6 (7), feature the tris(2-pyridyl) ligands coordinated through their three nitrogen atoms to *cis*-Mo(η^3 -methylalyl)(CO)₂ fragments. In these, the two carbonyl groups and the metal form acute angles (80.7(3)° in 6 and 84.14(18)° in 7) in agreement with the solution IR spectra

discussed above, and, accordingly, the methylalyl groups display an *exo* orientation. This contrasts with the geometry found in our compound [Mo(η^3 -methylalyl)(CO)₂][9]aneS₃][BAR'₄], in which the OC–Mo–CO is obtuse, and the methylalyl ligand is rotated.^[6] The difference can be attributed to the less steric demand of the tris(2-pyridyl) ligands compared with 1,4,7-trithiacyclononane.

The study of the behavior of compounds 6 and 7 towards several anions revealed a fundamental difference: the tris(2-pyridyl)methane compound 7 was stable; in contrast, the anions studied were found to coordi-

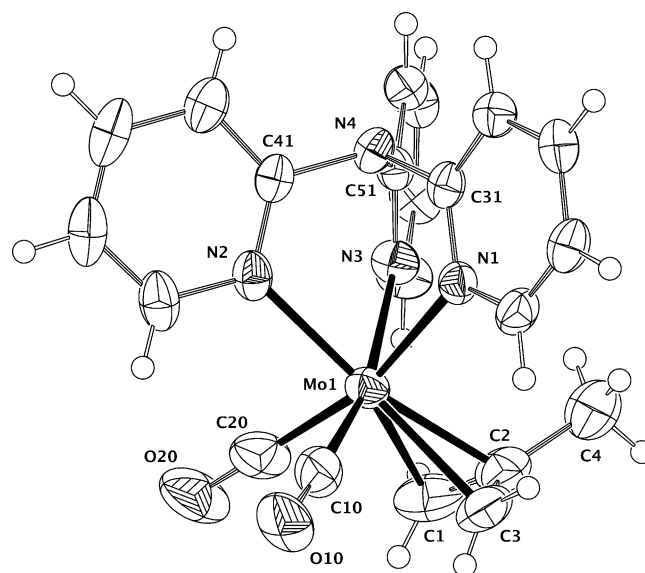


Figure 5. Thermal-ellipsoid (50%) plot of the cation of 6.

nate the molybdenum atom of 6, displacing one of the 2-pyridyl groups of the tris(2-pyridyl)amine ligand. These displacement reactions were instantaneous and monitoring with IR (featuring νCO bands significantly lower than those of the cationic precursor) and ^1H NMR spectroscopy failed to detect any intermediates. The resulting neutral complexes could be isolated for chloride (8), bromide (9) and methanesulfonate (10). In their solid-state structures, determined by X-ray diffraction and shown in Figure 4–6S (see the Supporting Information), one of the coordinated 2-pyridyl groups is *trans* to one carbonyl ligand, and the other, *trans* to the methylalyl group, the anionic ligand incorporated in the reaction is *trans* to the second carbonyl. Therefore, the structure is asymmetric. The room temperature ^1H NMR spectra of these neutral complexes reflect ap-

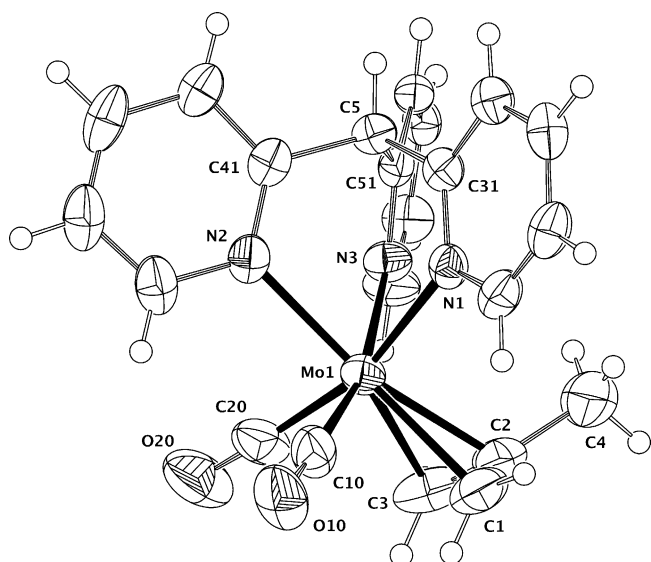


Figure 6. Thermal-ellipsoid (50%) plot of the cation of **7**.

parent molecular mirror planes. However, at low temperatures, the spectra reflect asymmetric structures like those found in the solid state (see Figure 7S in Supporting Information). Therefore, the room temperature spectra are attributed to the operation of a dynamic process, presumably a trigonal twist, which is slowed down at low temperatures.

When the product of the reaction between **6** and tetrabutylammonium methanesulfonate was crystallized by slow diffusion of hexane into a dichloromethane solution, two different types of crystals were obtained, one of them corresponding to the neutral complex **10** mentioned above. The second type of crystals was found to correspond to the hydrogen-bonded ion pair **11**. The structure of **11**, an isomer of **10**, is displayed in Figure 7 and consists of an intact cationic complex like that in compound **6**, with a non-coordinated methanesulfonate anion. The latter is hydrogen bonded through its oxygen atoms to the hydrogen atoms of the C–H groups in the 3-position of 2-pyridyl groups. Structurally, compound **11** resembles the hydrogen-bonded ion pairs formed between the cationic tris(2-pyridyl)methane complex from compound **7** and different anions, which will be discussed below. However, unlike those adducts that are stable in solution, and are the single products of the reactions between **7** and the tetrabutylammonium salts of several anions, compound **11** could only be isolated, accompanied by **10**, by slow crystallization, and only the neutral complex **10** could be spectroscopically detected when equimolar amounts of tetrabutylammonium methanesulfonate and compound **6** were mixed in dichloromethane. These results indicate that the formation of **10** is largely favored over that of **11**, and that the crystallization of **11** from the solutions in which **10** is the predominant (the only spectroscopically detected) product results from the low solubility of **11**. The fact that no analogs of **11** with other anions could be obtained, not even detected, is attributed to the higher nucleophilicity of chloride and bromide compared to methanesulfonate.

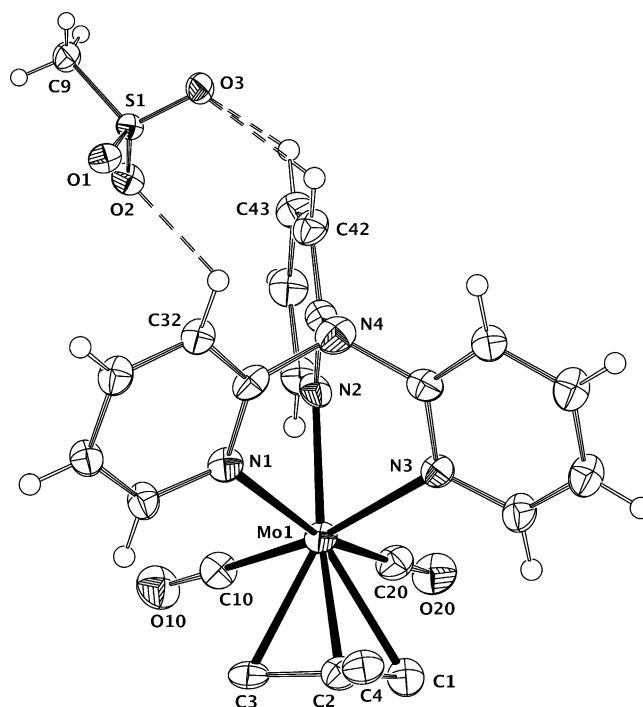


Figure 7. Thermal-ellipsoid (30%) plot of **11**. Main hydrogen bond distances (Å) and angles (°): C32–O2 3.535(0), C43–O3 3.173(0), C42–O3 3.171(0); C32–H32–O2 152.72(0), C43–H43–O3 133.55(0), C42–H42–O3 147.67(0).

The ion pairs formed by the cationic complex of **7** and chloride (**12**), bromide (**13**), iodide (**14**), nitrate (**15**) and perrhenate (**16**) could be isolated (see the Experimental Section) as pure crystalline solids, and their structures have been determined by X-ray diffraction. The results are displayed in Figures 8–12.

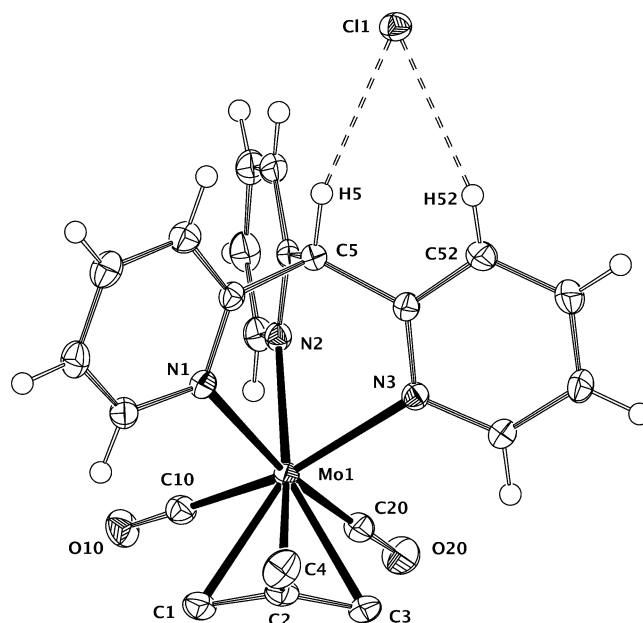


Figure 8. Thermal-ellipsoid (50%) plot of **12**. Main hydrogen bond distances (Å) and angles (°): C5–Cl1 3.593(0), C52–Cl1 3.488(0); C5–H5–Cl1 163.25(0), C52–H52–Cl1 151.11(0).

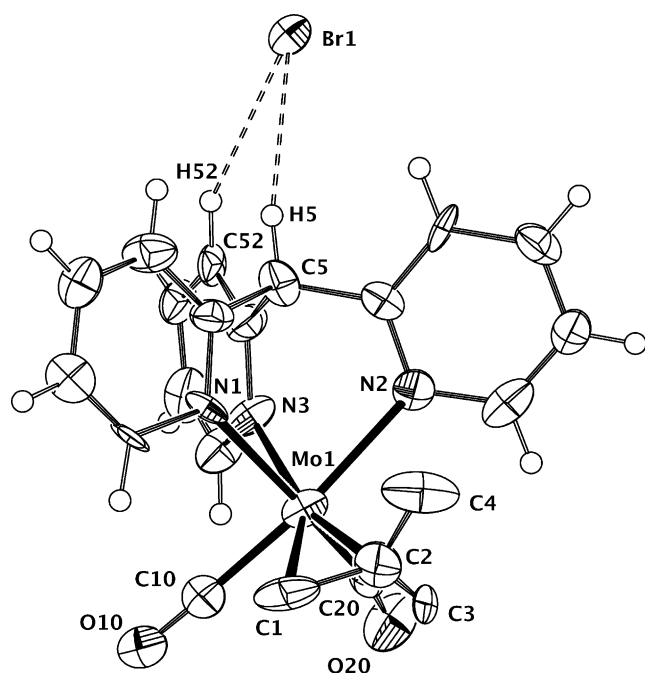


Figure 9. Thermal-ellipsoid (30%) plot of **13**. Main hydrogen bond distances (Å) and angles (°): C5–Br1 3.708(0), C52–Br1 3.722(0), C5–H5–Br1 159.97(1), C52–H52–Br1 150.99(1).

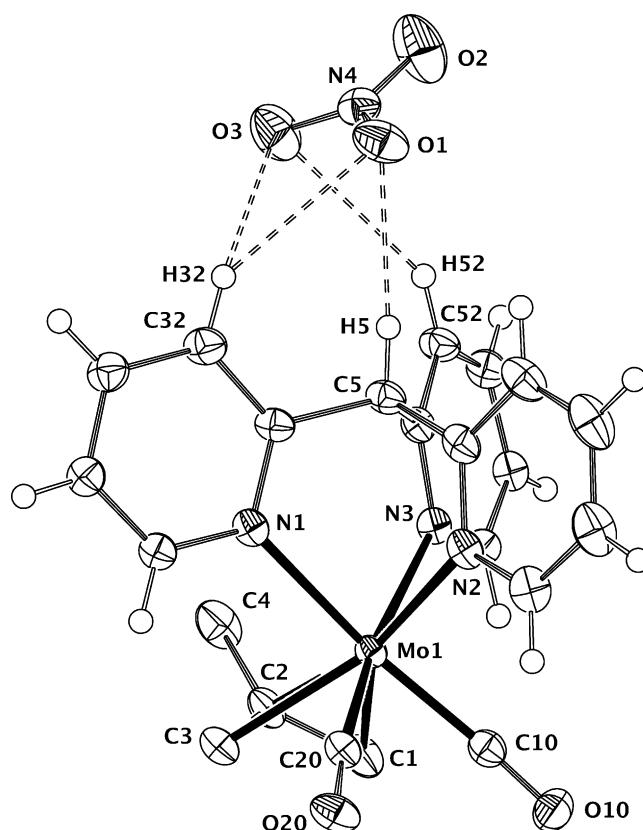


Figure 11. Thermal-ellipsoid (30%) plot of **15**. Main hydrogen bond distances (Å) and angles (°): C32–O1 3.478(0), C32–O3 3.405(0), C5–O1 3.305(0), C52–O3 3.585(0); C32–H32–O1 145.55(0), C32–H32–O3 143.03(0), C5–H5–O1 175.57(0), C52–H52–O3 148.44(0).

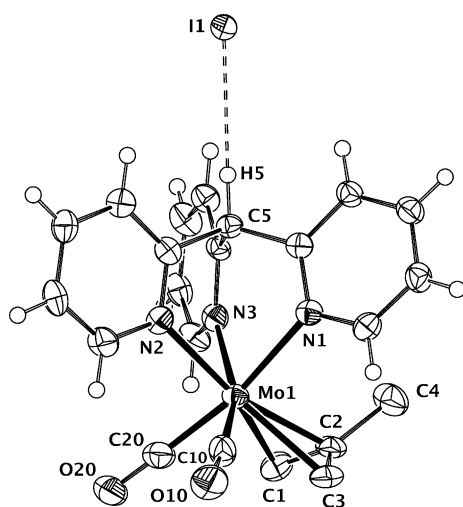


Figure 10. Thermal-ellipsoid (30%) plot of **14**. Main hydrogen bond distances (Å) and angles (°): C5–H1 3.890(0), C5–H5–H1 164.45(0).

In each case the anions approach the cationic complex so that the closer contacts are those with the C–H groups of the tris(2-pyridyl)methane ligand. Some of these contacts, consistent with weak hydrogen bonds, are marked with dashed lines in the ORTEP diagrams. In solution, the interactions between **7** and the anions were investigated by ^1H NMR spectroscopy. It was found that the signal of the bridgehead C–H group is the one that undergoes a more pronounced downfield shift when tetrabutylammonium chloride was added to a deuterated dichloromethane solution of **7**. Smaller shifts were found for the

2-pyridyl C(3)–H groups (See Figure 13). The signals corresponding to the C(6)–H did not experience an appreciable shift when four equivalents of Bu_4NCl were added. From these results it can be concluded that chloride approaches the cationic complex from the periphery of the tris(2-pyridyl)methane ligand, in line with the solid-state structures discussed above. Similar results were found with other anions (see the Supporting Information)

The Job plot for the interaction of **7** with chloride, using the chemical shift of the bridgehead CH group (Figure 14) indicates a 1:1 stoichiometry.

Discussion

Our results demonstrate that the cationic rhenium complex present in **1** is stable in the presence of the chloride anion in dichloromethane solution, i.e., that the $[\text{9}]_{\text{aneS}_3}$ ligand is not displaced by chloride, a nucleophilic anion in organic solvents of low solvating power. This stands in contrast with the easy displacement of the $[\text{9}]_{\text{aneS}_3}$ ligand by chloride in our recently reported molybdenum allyl cationic complexes,^[6] as well as with the Pd complex reported by the groups of Bedford and Tucker.^[4] Results by Elias, Wiegardt, and coworkers indicate that the manganese complex $\text{fac-}[\text{Mn}(\text{CO})_3([\text{9}]_{\text{aneS}_3})]^+$, analogous to **1**, is also stable in the presence of bromide and chlo-

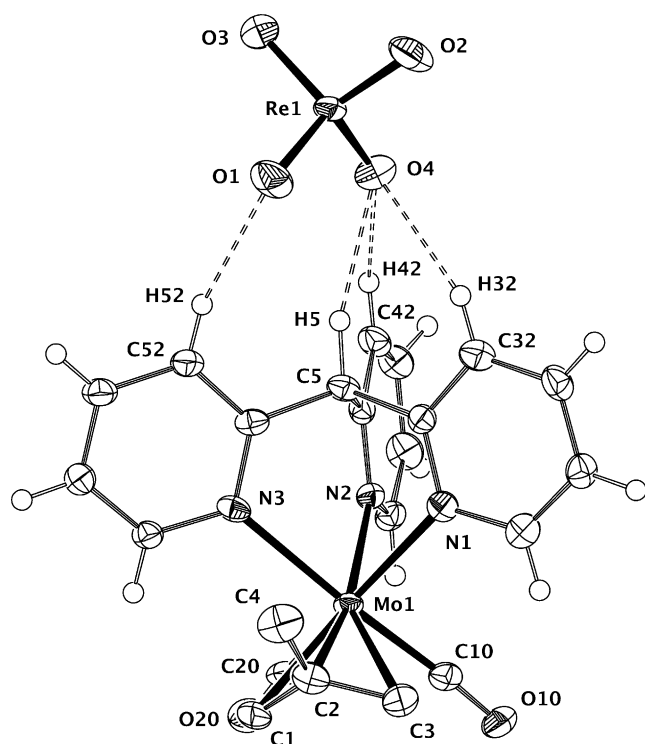


Figure 12. Thermal-ellipsoid (30) plot of **16**. Main hydrogen bond distances (Å) and angles (°): C3–O4 3.475(0), C42–O4 3.435(0), C5–O4 3.274(0), C52–O1 3.358(0); C32–H32–O4 140.17(0), C42–H42–O4 144.30(0), C5–H5–O4 160.25(0), C52–H52–O1 157.68(0).

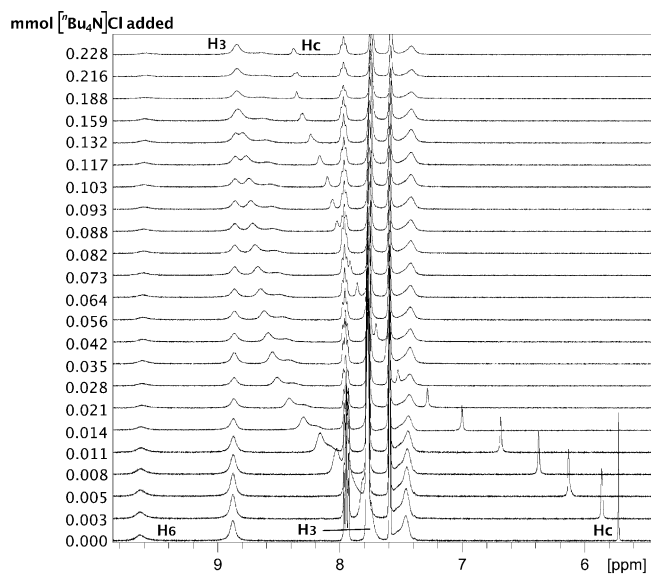


Figure 13. ^1H NMR spectral changes observed when **7** is treated with increasing amounts of $[\text{Bu}_4\text{N}]\text{Cl}$.

ride counteranions.^[19] The authors reported the preparation of $[\text{Mn}(\text{CO})_3([\text{9}]\text{aneS}_3)]\text{X}$ ($\text{X} = \text{Cl}, \text{Br}$) by reaction of $[\text{Mn}(\text{CO})_5\text{X}]$ with $[\text{9}]\text{aneS}_3$ in dimethylformamide and recrystallization of the product in acetonitrile. Following anion exchange with $[\text{Bu}_4\text{N}][\text{PF}_6]$, they isolated crystals of composition $[\text{Mn}(\text{CO})_3([\text{9}]\text{aneS}_3)]_3(\text{PF}_6)_3\text{Br}\cdot 2\text{H}_2\text{O}$, confirmed by X-ray diffraction.

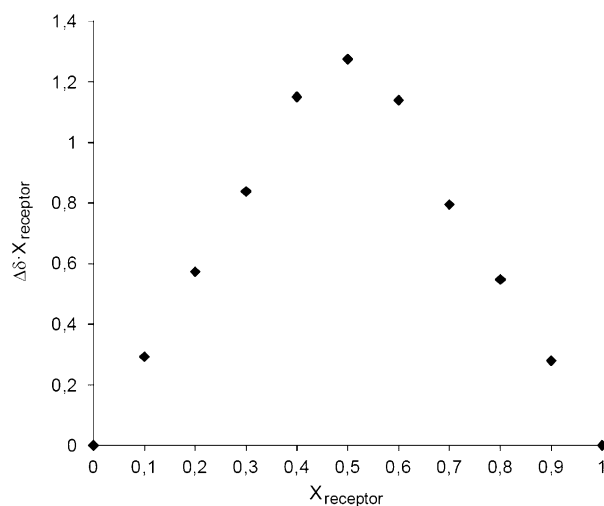


Figure 14. Job plot for the titration of **7** with Bu_4NCl .

Therefore, the presence of a third row metal (rhenium, in the case of compound **1**) is not a requisite for the stability of a cationic $[\text{9}]\text{aneS}_3$ complex in the presence of chloride or bromide. In the same line, cationic $[\text{9}]\text{aneS}_3$ Rh^{III} complexes are stable in the presence of chloride.^[20] The manganese and rhenium (I) complexes, as well as these rhodium (III) complexes, have a d^6 configuration, which contributes to the kinetic stability of the complexes, a feature that is not present in the d^4 molybdenum (II) complexes, or in the d^8 palladium (II) complexes, so perhaps the stability associated to a d^6 electronic configuration can be one factor contributing to their different substitution behavior towards chloride.

The reaction of **1** with tetrabutylammonium fluoride results in the formation of the dimeric complex **5**, in which thiolate ligands, generated by ring opening of the trithiacyclononane ligands, bridge the two rhenium atoms. The formation of **5** can be rationalized by the mechanism shown in Scheme 1, in which the key feature is the deprotonation by fluoride (or hydroxide, since the fluoride salt contains water) of one of the C–H groups of the cationic rhenium complex, and the concomitant C–S bond cleavage. The transformation of a cationic complex (in **1**) to the neutral complex **5** accounts for the large decrease in the wavenumber values of the IR ν_{CO} bands. Related deprotonations of positively charged d^6 complexes of $[\text{9}]\text{aneS}_3$, also involving C–S bond cleavage and formation of vinyl groups, have been demonstrated by Schröder, Wiegardt and coworkers for the homoleptic tricationic M^{III} $[\text{M}([\text{9}]\text{aneS}_3)_2]^{3+}$ ($\text{M} = \text{Co}, \text{Rh}, \text{Ir}$) coordination compounds^[21] and by Bennett and coworkers for the dicationic (arene)ruthenium (II) $[\text{Ru}(\eta^6\text{-C}_6\text{Me}_6)([\text{9}]\text{aneS}_3)]^{2+}$ organometallic complex.^[22] In these previous examples, the products were mononuclear complexes in which the three different sulfur atoms of the cleaved ligand remain bonded to the metal center. In contrast, in compound **5**, the sulfur bearing the vinyl group is uncoordinated, and the thiolate sulfur acts as a bridge.

Binding constants for the stable molybdenum tris(2-pyridyl)methane compound **7** (Table 1), calculated from the ^1H NMR titrations represented in Figure 15 and Supporting Information,

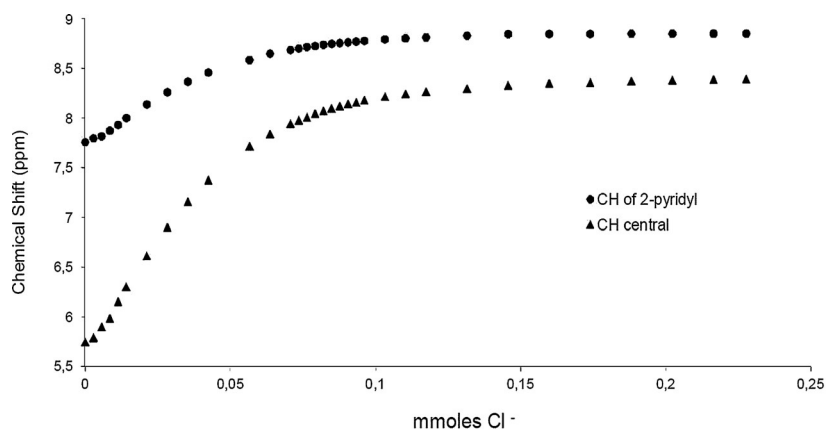


Figure 15. ^1H NMR titration profiles of **7** with Bu_4NCl .

were found to be very small compared with those found for the molybdenum^[6] and rhenium (compound **1**, see above) complexes of the [9]aneS₃ ligand. At least in part, the difference can be attributed to the presence of the sulfur atoms, electronegative and directly bonded to the cationic metal center, in the [9]aneS₃ complexes, which would increase the acidity of the adjacent C–H groups. In addition, in the complexes of the [9]aneS₃ ligand, an anion can interact simultaneously with three of the C–H *exo*-groups, whereas in the case of the tris(2-pyridyl) hosts, the solid state structures for chloride and bromide show that the significant interactions are with the C–H bridgehead group and with one of the aryl C–H groups (Figure 16).

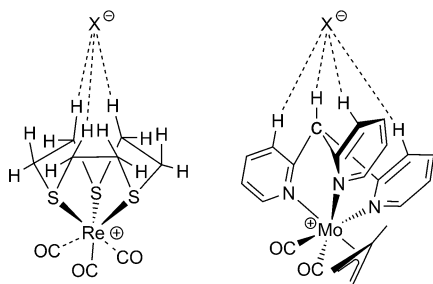


Figure 16. Host-anion binding.

In spite of their relatively low stability, shown by the small binding constants (Table 1), the ion pairs formed by the tris(2-pyridyl) molybdenum complexes with several anions, have been demonstrated to be stable to permit their isolation as pure crystalline solids.

The tris(2-pyridyl) complexes have been found to be inert against the displacement of the coordinated 2-pyridyl groups by anions, even in the presence of an excess of the relatively nucleophilic chloride anion in low-solvating dichloromethane, or for long periods of time, like those needed for slow diffusion crystallization (typically, several days). This behavior stands in sharp contrast to the easy substitution of one of the 2-pyridyl groups in the complex of tris(2-pyridyl)amine discussed above. A comparison of the data of the compounds **6** and **7**

does not shed light on the reasons of this dramatic difference. However, the structures of the neutral products **8**, **9**, and **10** provide an explanation: The coordination around the bridgehead nitrogen atom is planar, as indicated by the sum of the angles about it, 360° . Therefore, dissociation of one of the 2-pyridyl groups allows for the attaining of this planarity. Literature searches showed that planarity at the central nitrogen is always found in free tris(2-pyridyl)amine^[23] and related compounds

as well as in other metal complexes with bidentate tris(2-pyridyl)amine ligands,^[24] reflecting a more stable conformation. This higher stability can be traced to the delocalization of the nitrogen lone pair involving the aryl rings. These results suggest that, in general, complexes of the tris(2-pyridyl)amine will be less stable against substitution than those of, for instance, tris(2-pyridyl)methane, which lack lone pairs at the bridgehead atom.

Conclusion

Two types of metal-complex-based anion hosts have been synthesized, which are more stable against ligand substitution by anions than our previously reported allyldicarbonyl molybdenum-based hosts $[\text{Mo}(\eta^3\text{-methylallyl})(\text{CO})_2][\text{9]aneS}_3][\text{BAR}'_4]$ and $[\text{Mo}(\eta^3\text{-allyl})(\text{CO})_2][\text{9]aneS}_3][\text{BAR}'_4]$: rhenium tricarbonyl trithiacyclonane complexes, and allyldicarbonyl molybdenum complexes of tris(2-pyridyl)methane. Tris(2-pyridyl)amine analogs of the later have been found to undergo facile substitution of one of the 2-pyridyl groups by anions, presumably reflecting the tendency of tris(2-pyridyl)amine to become planar at nitrogen. Ion pairs formed between several simple inorganic anions and the stable cationic rhenium and molybdenum complexes could be isolated, and their solid state structures, determined by X-ray diffraction, show hydrogen bonding between C–H groups of the [9]aneS₃ or TpyCH ligands and the anions. Fluoride deprotonates the [9]aneS₃ ligand of the rhenium complex to afford a dimeric, thiolato-bridged complex. ^1H NMR spectroscopy demonstrates that the interactions between the anions and the C–H groups at the periphery of the cationic complexes persist in dichloromethane solution, and allowed to establish the 1:1 stoichiometry of the adducts, and to calculate the binding constants. Binding constants have been found to be larger for the rhenium hosts.

Experimental Section

All manipulations were carried out at room temperature under a dinitrogen atmosphere employing Schlenk techniques. CH_2Cl_2 was dried over CaH_2 , diethylether over Na-benzophenone, and hexane and toluene over sodium. IR and NMR spectra were recorded on

Perkin–Elmer FT1720-X and Bruker AV-400 or AV-300 spectrometers respectively. Deuterated solvents were degassed by three freeze-pump-thaw cycles, dried over 4 Å molecular sieves and stored in the dark. $[\text{ReBr}(\text{CO})_3]^{[25]}$ and $[\text{MoCl}(\eta^3\text{-methallyl})(\text{CO})_2(\text{NCMe})_2]^{[18]}$ (methallyl = $\text{C}_3\text{H}_4\text{-Me-2}$) were prepared according to literature procedures. All other chemicals were purchased and used without further purification. The characterization labeling Scheme is shown in Figure 17.

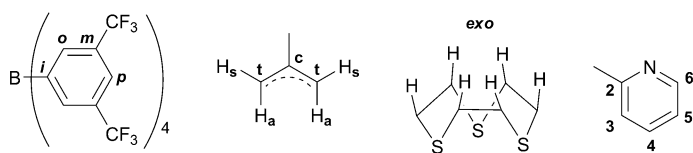


Figure 17. Labeling Scheme for BAR'_4 , methallyl, *exo* hydrogens of [9]ane S_3 and 2-pyridyl.

$[\text{Re}(\text{CO})_3(\text{[9]aneS}_3)][\text{BAR}'_4]$ (1): A mixture of $[\text{ReBr}(\text{CO})_3]$ (0.250 g, 0.610 mmol) and [9]ane S_3 (0.111 g, 0.610 mmol) was heated to reflux in toluene for 1 h. The solution was allowed to reach room temperature obtaining a white precipitate. After removal of toluene the solid was dried in vacuo and dissolved in CH_2Cl_2 (30 mL) and NaBAR'_4 (0.540 g, 0.610 mmol) was added. The reaction mixture was stirred at room temperature overnight. After filtration through diatomaceous earth the filtrate was reduced to 5 mL. Addition of hexane resulted in the formation of a microcrystalline white solid which was washed with hexane (3×10 mL) and dried under reduced pressure. Yield: 0.682 g, 85%. $^1\text{H NMR}$ (400 MHz, CD_2Cl_2): $\delta = 7.79$ (s, 8H; H_o of BAR'_4), 7.64 (s, 4H; H_p of BAR'_4), 3.05 (m, 6H; CH_2 of [9]ane S_3), 2.74 ppm (m, 6H; CH_2 of [9]ane S_3); $^{13}\text{C}\{^1\text{H}\}$ NMR (100 MHz, CD_2Cl_2): $\delta = 186.4$ (s, CO), 161.7 (c, $J(\text{C}, \text{B}) = 50.2$ Hz, C_i of BAR'_4), 134.7 (s, C_o of BAR'_4), 128.7 (m, C_m of BAR'_4), 124.6 (c, $J(\text{C}, \text{F}) = 272.7$ Hz, CF_3 of BAR'_4), 117.5 (s, C_p of BAR'_4), 34.5 ppm (s, CH_2 of [9]ane S_3); IR (CH_2Cl_2) $\tilde{\nu} = 2058$ (vs), 1974 cm^{-1} (s); elemental analysis calcd (%) for $\text{C}_{41}\text{H}_{24}\text{BF}_{24}\text{O}_3\text{ReS}_3$ (1313.80): C 37.44, H 1.84; found: C 37.59, H 2.03.

$[\text{Re}(\text{CO})_3(\text{[9]aneS}_3)]\text{-Cl}$ (2): A solution of **1** (0.100 g, 0.076 mmol) and $[\text{nBu}_4\text{N}]\text{Cl}$ (0.021 g, 0.076 mmol) in CH_2Cl_2 (10 mL) was stirred for 30 min. After evaporation of the solvent, the white residue was washed with diethylether (3×5 mL) (to remove the $[\text{nBu}_4\text{N}][\text{BAR}'_4]$ salt) and dried in vacuo. By slow diffusion of hexane into a concentrated solution of **2** in CH_2Cl_2 at -20°C , colorless crystals of good quality (0.036 g, 88%) for the determination of the structure by X-ray analysis were obtained. $^1\text{H NMR}$ (400 MHz, CD_2Cl_2): $\delta = 4.00$ (m, 6H, CH_2 of [9]ane S_3), 2.96 ppm (m, 6H, CH_2 of [9]ane S_3); $^{13}\text{C}\{^1\text{H}\}$ NMR (100 MHz, CD_2Cl_2): $\delta = 188.2$ (s; CO), 35.9 ppm (s; CH_2 of [9]ane S_3); IR (CH_2Cl_2): $\tilde{\nu} = 2050$ (vs), 1961 cm^{-1} (s); elemental analysis calcd (%) for $\text{C}_9\text{H}_{12}\text{ClO}_3\text{ReS}_3 \cdot 3\text{H}_2\text{O}$ (540.08): C 22.23, H 2.49; found: C 22.55, H 2.54.

$[\text{Re}(\text{CO})_3(\text{[9]aneS}_3)]\text{-Br}$: This compound was prepared in a similar way to **2** starting from **1** (0.100 g, 0.076 mmol) and $[\text{nBu}_4\text{N}]\text{Br}$ (0.024 g, 0.076 mmol) to yield 0.031 g (77%). $^1\text{H NMR}$ (300 MHz, CD_2Cl_2): $\delta = 3.85$ (m, 6H; CH_2 of [9]ane S_3), 2.98 ppm (m, 6H; CH_2 of [9]ane S_3); IR (CH_2Cl_2) $\tilde{\nu} = 2051$ (vs), 1962 cm^{-1} (s); elemental analysis calcd (%) for $\text{C}_9\text{H}_{12}\text{BrO}_3\text{ReS}_3$ (530.48) C 20.38, H 2.28; found: C 20.05, H 2.42.

$[\text{Re}(\text{CO})_3(\text{[9]aneS}_3)]\text{-[CH}_3\text{SO}_3]$ (3): This compound was prepared as described above for **2** starting from **1** (0.100 g, 0.076 mmol) and $[\text{nBu}_4\text{N}][\text{CH}_3\text{SO}_3]$ (0.026 g, 0.076 mmol) to yield colorless crystals (0.034 g, 79%), one of which was used for an X ray analysis. $^1\text{H NMR}$ (400 MHz, CD_2Cl_2): $\delta = 3.61$ (m, 6H; CH_2 of [9]ane S_3), 2.96

(m, 6H; CH_2 of [9]ane S_3), 2.59 ppm (s, 3H; CH_3SO_3); IR (CH_2Cl_2) $\tilde{\nu} = 2050$ (vs), 1962 cm^{-1} (s); elemental analysis calcd (%) for $\text{C}_{10}\text{H}_{15}\text{O}_6\text{ReS}_4 \cdot \text{H}_2\text{O}$ (563.69): C 21.31, H 3.04; found: C 21.40, H 3.08.

Reaction of **1 with $[\text{nBu}_4\text{N}]\text{F} \cdot 3\text{H}_2\text{O}$:** A solution of **1** (0.100 g, 0.076 mmol) and $[\text{nBu}_4\text{N}]\text{F} \cdot 3\text{H}_2\text{O}$ (0.023 g, 0.076 mmol) in CH_2Cl_2 (10 mL) was stirred for 30 min. The IR of the reaction crude at this point shows the presence of several species. The solvent was evaporated and the white solid residue was extracted with diethylether (3×10 mL). The white solid insoluble in ether was found to be $[\text{Re}(\text{CO})_3(\text{[9]aneS}_3)]\text{-F}$ (**4**). Yield: 0.999 g, 28%. $^1\text{H NMR}$ (400 MHz, CD_2Cl_2): $\delta = 3.75$ (m, 6H; CH_2 of [9]ane S_3), 2.94 ppm (m, 6H; CH_2 of [9]ane S_3); Limited solubility precluded the acquisition of its ^{13}C NMR spectrum; IR (CH_2Cl_2) $\tilde{\nu} = 2050$ (vs), 1961 cm^{-1} (s); elemental analysis calcd (%) for $\text{C}_9\text{H}_{12}\text{FO}_3\text{ReS}_3$ (469.58): C 23.02, H 2.58; found: C 23.11, H 2.63. The ether washings were collected, the solvent was evaporated and the resulting solid was found to contain **5**, $[\text{nBu}_4\text{N}][\text{BAR}'_4]$ and some non-identified compounds.

Crystallization from CH_2Cl_2 /hexane afforded solids enriched in **5**. $^1\text{H NMR}$ (400 MHz, CD_2Cl_2): $\delta = 6.43$ (m, 2H; CH), 5.25 (m, 4H; CH_2 terminal), 3.15–2.90 ppm (m, 16H; CH_2); IR (CH_2Cl_2) $\tilde{\nu} = 2013$ (vs), 1917 cm^{-1} (s). However, **5** was always contaminated with non-identified compounds and we have been unable to obtain spectroscopically pure samples. Repeated attempts to purify **5** by crystallization failed to provide samples of analytical purity, or amounts of crystals enough for NMR samples. Our crystal resulting from one of these crystallizations (slow diffusion of hexane into a concentrated solution of **5** was used for the structural characterization by X-ray diffraction.

$[\text{Mo}(\eta^3\text{-methallyl})(\text{CO})_2(\text{TpyN})][\text{BAR}'_4]$ (6): A mixture of $[\text{MoCl}(\eta^3\text{-methallyl})(\text{CO})_2(\text{MeCN})_2]$ (0.110 g, 0.339 mmol), TpyN (0.084 g, 0.339 mmol) and NaBAR'_4 (0.300 g, 0.339 mmol) in CH_2Cl_2 (15 mL) was stirred for 1 h. After filtration through diatomaceous earth the filtrate was reduced to 5 mL. Addition of hexane resulted in the formation of orange crystals (2 days at -20°C), one of which was used for X-ray analysis (0.350 g, 78%). $^1\text{H NMR}$ (300 MHz, CD_2Cl_2): $\delta = 9.54$ (s_{br} , 1H; H_{py}), 9.05 (s_{br} , 2H; H_{py}), 8.04 (m, 3H; H_{py}), 7.85 (m, 11H; 8H_o of BAR'_4 and 3H_{py}), 7.56 (m, 7H; 4H_p of BAR'_4 and 3H_{py}), 3.65 (s, 2H; H_{syn}), 1.87 (s, 2H; H_{anti}), 1.56 ppm (s, 3H; CH_3 of methallyl); $^{13}\text{C}\{^1\text{H}\}$ NMR (75 MHz, CD_2Cl_2): $\delta = 227.5$ (s; CO), 164.5 (c, $J(\text{C}, \text{B}) = 49.8$ Hz; C_i of BAR'_4), 155.8 (s; py), 146.3 (s; py), 137.2 (s; C_o of BAR'_4), 131.3 (m; C_m of BAR'_4), 129.2 (s, 2C; py), 128.7 (s; py), 126.9 (c $J(\text{C}, \text{F}) = 272.5$; CF_3 of BAR'_4), 119.9 (s; C_p of BAR'_4), 88.4 (s; C_c of methallyl), 64.9 (s; C_t of methallyl), 20.5 ppm (s; CH_3 of methallyl); IR (CH_2Cl_2) $\tilde{\nu} = 1957$ (vs), 1872 cm^{-1} (s); elemental analysis calcd (%) for $\text{C}_{53}\text{H}_{31}\text{BF}_{24}\text{MoN}_4\text{O}_2 \cdot \text{CH}_2\text{Cl}_2$ (1403.50) C 46.15, H 2.37; N, 3.99; found: C 45.93, H 2.46, N 4.11.

$[\text{Mo}(\eta^3\text{-methallyl})(\text{CO})_2(\text{TpyCH})][\text{BAR}'_4]$ (7): A mixture of $[\text{MoCl}(\eta^3\text{-methallyl})(\text{CO})_2(\text{MeCN})_2]$ (0.080 g, 0.245 mmol), TpyCH (0.060 g, 0.245 mmol) and NaBAR'_4 (0.215 g, 0.245 mmol) in CH_2Cl_2 (15 mL) was stirred for 1 h. After filtration through diatomaceous earth, the solvent was removed in vacuo. The orange residue was washed with hexane (3×10 mL). By slow diffusion of hexane into a concentrated solution of **7** in CH_2Cl_2 at -20°C orange crystals were obtained (0.190 g, 60%), one of which was used for X-ray analysis. $^1\text{H NMR}$ (300 MHz, CD_2Cl_2): $\delta = 9.71$ (s_{br} , 1H; H_6 py $_{trans}$), 8.91 (s, 2H; H_6 py $_{cis}$), 7.93 (td, $J = 7.7, 1.6$ Hz, 3H; H_{py}), 7.83 (s, 8H; H_o of BAR'_4), 7.76 (d, $J = 5.9$ Hz, 3H; H_{py}), 7.64 (s, 4H; H_p of BAR'_4), 7.47 (s_{br} , 3H; H_{py}), 5.75 (s, 1H; C–H), 3.61 (s, 2H; H_{syn}), 1.98 (s, 2H; H_{anti}), 1.82 ppm (s, 3H; CH_3 of methallyl); $^{13}\text{C}\{^1\text{H}\}$ NMR (75 MHz, CD_2Cl_2): $\delta = 229.2$ (s; CO), 163.4 (c $J(\text{C}, \text{B}) = 49.8$ Hz; C_i of BAR'_4), 159.5 (s; py), 156.7 (s; py), 155.9 (s; py), 144.8 (s; py), 144.2 (s; py), 137.0 (s; C_o of BAR'_4),

131.6 (m; C_m of BAR'_4), 129.6 (s; py), 127.3 (s; py), 127.2 (s; py), 126.9 (c, $J(C,F)=272.5$; CF_3 of BAR'_4), 119.9 (s; C_p of BAR'_4), 91.3 (s; C_c of methallyl), 66.7 (s; C_t of methallyl), 63.1 (s; C–H), 20.9 ppm (s; CH_3 of methallyl); IR (CH_2Cl_2) $\tilde{\nu}=1955$ (vs), 1867 cm^{-1} (s); elemental analysis calcd (%) for $C_{54}H_{32}BF_{24}MoN_3O_2$ (1317.58): C 49.12, H 2.44, N 3.18; found: C 49.24, H 2.40; N 3.06.

[MoCl(η^3 -methallyl)(CO) $_2$ (TpyN)] (8): Method A) A solution of **6** (0.100 g, 0.076 mmol) and $[nBu_4N]Cl$ (0.021 g, 0.076 mmol) was stirred for 30 min. The solvent was removed under vacuum and the resulting yellow residue was washed with diethylether (3 \times 10 mL) and dried in vacuo. By slow diffusion of hexane into a concentrated solution of **8** in CH_2Cl_2 at $-20^\circ C$ yellow crystals of good quality (0.030 g, 80%) for the determination of the structure by X-ray analysis were obtained. 1H NMR (300 MHz, CD_2Cl_2): 8.85 (d, $J=4.7$ Hz, 2H; $H_{py\ coord}$), 8.35 (d, $J=3.9$ Hz, 1H; $H_{py\ uncoord}$), 7.89 (m, 4H; $2H_{py\ coord}$ and $2H_{py\ uncoord}$), 7.72 (m, 1H; $H_{py\ uncoord}$), 7.37 (s, 2H; $H_{py\ coord}$), 7.06 (m, 2H; $H_{py\ coord}$), 3.07 (s, 2H; H_{syn}), 2.59 (s, 3H; CH_3 of methallyl), 1.26 ppm (s, 2H; H_{anti}); $^{13}C\{^1H\}$ NMR (75 MHz, CD_2Cl_2): $\delta=226.8$ (s; CO), 154.3 (s; py), 152.5 (s; py), 152.0 (s; py), 147.6 (s; py), 139.0 (s; py), 138.2 (s; py), 124.0 (s; py), 122.4 (s; py), 118.1 (s; py), 110.4 (s; py), 83.7 (s; C_c of methallyl), 57.1 (s; C_t of methallyl), 20.9 ppm (s; CH_3 of methallyl); IR (CH_2Cl_2) $\tilde{\nu}=1934$ (vs), 1842 cm^{-1} (s); elemental analysis calcd (%) for $C_{21}H_{19}ClMoN_4O_2$ (490.80): C 51.39, H 3.90, N 11.42; found: C 51.18, H 3.78, N 11.27. Method B) A mixture of $[MoCl(\eta^3\text{-methallyl})(CO)_2(MeCN)_2]$ (0.030 g, 0.092 mmol) and TpyN (0.023 g, 0.092 mmol) in CH_2Cl_2 (15 mL) was stirred for 3 h. Spectroscopic and analytical data of the product obtained agree with those obtained by method A.

[MoBr(η^3 -methallyl)(CO) $_2$ (TpyN)] (9): A mixture of **6** (0.100 g, 0.076 mmol) and $[nBu_4N]Br$ (0.024 g, 0.076 mmol) was stirred for 30 min. After evaporation of the solvent under vacuum, the residue was washed with diethylether (3 \times 5 mL), dried in vacuo and the resulting solid was dissolved in CH_2Cl_2 . This solution was layered with hexane (20 mL) and orange crystals were obtained from slow diffusion at $-20^\circ C$. (0.033 g, 82%). 1H NMR (400 MHz, CD_2Cl_2): $\delta=9.02$ (d, $J=5.0$ Hz, 2H; $H_{py\ coord}$), 8.34 (d, $J=3.8$ Hz, 1H; $H_{py\ uncoord}$), 8.02 (m, 2H; $H_{py\ coord}$), 7.87 (s, 1H; $H_{py\ uncoord}$), 7.86 (s, 1H; $H_{py\ uncoord}$), 7.71 (m, 1H; $H_{py\ uncoord}$), 7.36 (m, 2H; $H_{py\ coord}$), 7.05 (m, 2H; $H_{py\ coord}$), 3.13 (s, 2H; H_{syn}), 2.68 (s, 3H; CH_3 of methallyl), 1.27 ppm (s, 2H; H_{anti}); $^{13}C\{^1H\}$ NMR (100 MHz, CD_2Cl_2): $\delta=226.6$ (s; CO), 154.3 (s; py), 152.9 (s; py), 152.5 (s; py), 147.6 (s; py), 139.1 (s; py), 138.2 (s; py), 124.0 (s; py), 122.3 (s; py), 118.1 (s; py), 110.4 (s; py), 83.5 (s; C_c of methallyl), 56.9 (s; C_t of methallyl), 21.7 ppm (s; CH_3 of methallyl); IR (CH_2Cl_2) $\tilde{\nu}=1937$ vs, 1847 cm^{-1} (s); elemental analysis calcd (%) for $C_{21}H_{19}BrMoN_4O_2$ (535.25): C 47.12, H 3.58, N 10.47; found: C 47.21, H 3.68, N 10.66.

[Mo(CH $_3$ SO $_3$)(η^3 -methallyl)(CO) $_2$ (TpyN)] (10): This compound was prepared in a similar way to **8** starting from **6** (0.100 g, 0.076 mmol) and $[nBu_4N][CH_3SO_3]$ (0.026 g, 0.076 mmol) to yield orange crystals (0.036 g, 75%), one of which was used for X-ray analysis. 1H NMR (400 MHz, CD_2Cl_2): $\delta=8.92$ (d, $J=5.0$ Hz, 2H; $H_{py\ coord}$), 8.34 (s_{br} , 1H; $H_{py\ uncoord}$), 7.94 (m, 4H; $2H_{py\ coord}$ and $2H_{py\ uncoord}$), 7.73 (m, 1H; $H_{py\ uncoord}$), 7.43 (m, 2H; $H_{py\ coord}$), 7.05 (m, 2H; $H_{py\ coord}$), 3.48 (s, 2H; H_{syn}), 2.63 (s, 3H; CH_3 of methallyl), 2.50 (s, 3H; CH_3SO_3), 1.29 ppm (s, 2H; H_{anti}); $^{13}C\{^1H\}$ NMR (100 MHz, CD_2Cl_2): $\delta=227.5$ (s; CO), 154.1 (s; py), 152.1 (s; py), 151.3 (s; py), 147.6 (s; py), 139.3 (s; py), 138.3 (s; py), 124.4 (s; py), 122.6 (s; py), 118.3 (s; py), 110.4 (s; py), 83.7 (s; C_c of methallyl), 57.1 (s; C_t of methallyl), 40.5 (s; CH_3SO_3) 20.9 ppm (s; CH_3 of methallyl); IR (CH_2Cl_2) $\tilde{\nu}=1942$ (vs), 1848 cm^{-1} (s); elemental analysis calcd (%) for $C_{22}H_{22}MoN_4O_5S\cdot CH_2Cl_2$ (635.37): C 43.47, H 3.81, N 8.82; found: C 43.21, H 3.61, N 8.56.

[Mo(η^3 -methallyl)(CO) $_2$ (TpyCH)]-Cl (12): A mixture of **7** (0.050 g, 0.038 mmol) and $[nBu_4N]Cl$ (0.014 g, 0.038 mmol) in CH_2Cl_2 (15 mL) was stirred for 30 min. After evaporation of the solvent under vacuum the resulting yellow residue was washed with diethylether (3 \times 10 mL) (to remove the $[nBu_4N][BAR'_4]$ salt) and dried in vacuo. By slow diffusion of hexane into a concentrated solution of **12** in CH_2Cl_2 at $-20^\circ C$, yellow crystals of good quality (0.016 g, 86%) for the determination of the structure by X-ray analysis were obtained. 1H NMR (300 MHz, CD_2Cl_2): $\delta=9.59$ (s_{br} , 1H; H_{py}), 8.89 (s_{br} , 5H; H_{py}), 8.54 (s, 1H; C–H), 7.99 (t (8.0), 3H; H_{py}), 7.43 (s_{br} , 3H; H_{py}), 3.58 (s, 2H; H_{syn}), 1.86 (s, 2H; H_{anti}), 1.71 ppm (s, 3H; CH_3 of methallyl); $^{13}C\{^1H\}$ NMR (75 MHz, CD_2Cl_2): 226.7 (s; CO), 155.6 (s; py), 151.9 (s; py), 141.9 (s; py), 128.7 (s; py), 123.9 (s; py), 88.6 (s; C_c of methallyl), 64.1 (s; C_t of methallyl), 56.8 (s; C–H), 19.2 ppm (s; CH_3 of methallyl); IR (CH_2Cl_2) $\tilde{\nu}=1950$ (vs), 1860 cm^{-1} (s); elemental analysis calcd (%) for $C_{22}H_{20}ClMoN_3O_2$ (489.81): C 53.95; H 4.11, N 8.58; found: C 54.10, H 4.23, N 8.78.

[Mo(η^3 -methallyl)(CO) $_2$ (TpyCH)]-Br (13): This compound was prepared as described above for **12** starting from **7** (0.100 g, 0.076 mmol) and $[nBu_4N]Br$ (0.024 g, 0.076 mmol) to yield orange crystals (0.033 g, 81%), one of which was used for an X ray analysis. 1H NMR (400 MHz, CD_2Cl_2): $\delta=9.60$ (s_{br} , 1H; H_{py}), 8.86 (s_{br} , 2H; H_{py}), 8.77 (s_{br} , 2H; H_{py}), 8.58 (s_{br} , 1H; H_{py}), 8.37 (s, 1H; C–H), 8.01 (t (7.7), 3H; H_{py}), 7.43 (s_{br} , 3H; H_{py}), 3.58 (s, 2H; H_{syn}), 1.87 (s, 2H; H_{anti}), 1.72 ppm (s, 3H; CH_3 of methallyl); $^{13}C\{^1H\}$ NMR (100 MHz, CD_2Cl_2): $\delta=226.7$ (s; CO), 155.4 (s; py), 151.9 (s; py), 141.1 (s; py), 128.5 (s; py), 123.9 (s; py), 88.7 (s; C_c of methallyl), 64.1 (s; C_t of methallyl), 56.7 (s; C–H), 19.2 ppm (s; CH_3 of methallyl); IR (CH_2Cl_2) $\tilde{\nu}=1951$ (vs), 1862 cm^{-1} (s); elemental analysis calcd (%) for $C_{22}H_{20}BrMoN_3O_2$ (534.26): C 49.46, H 3.77, N 7.86; found: C 49.50, H 3.86, N 8.09.

[Mo(η^3 -methallyl)(CO) $_2$ (TpyCH)]-I (14): $[nBu_4N]I$ (0.014 g, 0.038 mmol) was added to a solution of **7** (0.050 g, 0.038 mmol) in CH_2Cl_2 (15 mL) and the reaction mixture was stirred for 30 min. The rest of the procedure is similar to that described for **11**, including the solid-state determination by means of X-ray analysis. Yield: 0.019 g, 86%. 1H NMR (300 MHz, CD_2Cl_2): $\delta=9.63$ (s_{br} , 1H; H_{py}), 8.83 (s_{br} , 5H; H_{py}), 8.02 (t (7.6), 3H; H_{py}), 7.99 (s, 1H; C–H), 7.45 (s_{br} , 3H; H_{py}), 3.58 (s, 2H; H_{syn}), 1.89 (s, 2H; H_{anti}), 1.74 ppm (s, 3H; CH_3 of methallyl); $^{13}C\{^1H\}$ NMR (75 MHz, CD_2Cl_2): $\delta=226.6$ (s; CO), 155.1 (s; py), 152.5 (s; py), 141.2 (s; py), 124.1 (s; py), 124.1 (s; py), 89.0 (s; C_c of methallyl), 64.3 (s; C_t of methallyl), 56.8 (s; C–H), 19.3 ppm (s; CH_3 of methallyl); IR (CH_2Cl_2) $\tilde{\nu}=1952$ (vs), 1862 cm^{-1} (s); elemental analysis calcd (%) for $C_{22}H_{20}IMoN_3O_2$ (581.26): C 45.46, H 3.47, N 7.23; found: C 45.23, H 3.44, N 7.31.

[Mo(η^3 -methallyl)(CO) $_2$ (TpyCH)]-[CH $_3$ SO $_3$]: The procedure is similar to that described for the other adducts, but starting from **7** (0.100 g, 0.076 mmol) and $[nBu_4N][CH_3SO_3]$ (0.026 g, 0.076 mmol). Yield: 0.035 g, 84%. 1H NMR (400 MHz, CD_2Cl_2): $\delta=9.61$ (s_{br} , 1H; H_{py}), 8.82 (s_{br} , 2H; H_{py}), 8.69 (s_{br} , 1H; H_{py}), 8.58 (s_{br} , 2H; H_{py}), 8.02 (t (7.4), 3H; H_{py}), 7.43 (s, 4H; $3H_{py}$ and C–H), 3.65 (s, 2H; H_{syn}), 2.84 (s, 3H; CH_3SO_3), 1.89 (s, 2H; H_{anti}), 1.66 ppm (s, 3H; CH_3 of methallyl); $^{13}C\{^1H\}$ NMR (100 MHz, CD_2Cl_2): $\delta=226.7$ (s; CO), 155.2 (s; py), 151.9 (s; py), 141.4 (s; py), 128.7 (s; py), 123.9 (s; py), 88.8 (s; C_c of methallyl), 64.0 (s; C_t of methallyl), 58.4 (s; C–H), 39.7 (s; CH_3SO_3), 19.3 ppm (s; CH_3 of methallyl); IR (CH_2Cl_2) $\tilde{\nu}=1951$ (vs), 1862 cm^{-1} (s); elemental analysis calcd (%) for $C_{23}H_{23}MoN_3O_5S$ (549.45): C 50.27, H 4.21, N 7.65; found: C 50.18, H 4.33, N 7.59.

[Mo(η^3 -methallyl)(CO) $_2$ (TpyCH)]-[NO $_3$] (15): It was synthesized in a similar way than **12**, starting from **7** (0.050 g, 0.038 mmol) and $[nBu_4N][NO_3]$ (0.012 g, 0.038 mmol). By slow diffusion of hexane into a concentrated solution of **15** in CH_2Cl_2 yellow crystals were obtained for an X-ray analysis. Yield: 0.016 g, 81%. 1H NMR (300 MHz, CD_2Cl_2): $\delta=9.61$ (s_{br} , 1H; H_{py}), 8.87 (s_{br} , 2H; H_{py}), 8.46 (s_{br}

3H; H_{py}), 8.02 (t (7.8), 3H; H_{py}), 7.45 (s, 3H; H_{py}), 7.26 (s, C–H), 3.59 (s, 2H; H_{syn}), 1.89 (s, 2H; H_{anti}), 1.75 ppm (s, 3H; CH_3 of methallyl); $^{13}C\{^1H\}$ NMR (75 MHz, CD_2Cl_2): δ = 226.7 (s; CO), 154.9 (s; py), 152.1 (s; py), 141.4 (s; py), 128.2 (s; py), 124.1 (s; py), 89.2 (s; C_c of methallyl), 64.3 (s; C_t of methallyl), 59.3 (s; C–H), 19.4 ppm (s; CH_3 of methallyl); IR (CH_2Cl_2) $\tilde{\nu}$ = 1952 (vs), 1862 cm^{-1} (s); elemental analysis calcd (%) for $C_{22}H_{20}MoN_4O_5$ (516.36): C 51.17, H 3.90, N 10.85; found: C 51.32, H 3.80, N 10.49.

[Mo(η^3 -methallyl)(CO) $_2$ (TpyCH)] \cdot [ReO $_4$] (16): As it was described above, starting from **7** (0.050 g, 0.038 mmol) and $[nBu_4N][ReO_4]$ (0.012 g, 0.038 mmol), yellow crystals of good quality (0.022 g, 73%) for the determination of the structure of **16** by X-ray analysis were obtained. 1H NMR (300 MHz, CD_2Cl_2): δ = 9.61 (s_{br} , 1H; H_{py}), 8.88 (s_{br} , 2H; H_{py}), 8.23 (s_{br} , 3H; H_{py}), 8.05 (t (7.7), 3H; H_{py}), 7.49 (s_{br} , 3H; H_{py}), 6.56 (s, C–H), 3.59 (s, 2H; H_{syn}), 1.91 (s, 2H; H_{anti}), 1.78 ppm (s, 3H; CH_3 of methallyl); $^{13}C\{^1H\}$ NMR (75 MHz, CD_2Cl_2): δ = 226.6 (s; CO), 154.3 (s; py), 152.4 (s; py), 141.6 (s; py), 127.8 (s; py), 124.4 (s; py), 89.8 (s; C_c of methallyl), 64.5 (s; C_t of methallyl), 60.9 (s; C–H), 19.5 ppm (s; CH_3 of methallyl); IR (CH_2Cl_2) $\tilde{\nu}$ = 1953 (vs), 1864 cm^{-1} (s); elemental analysis calcd (%) for

$C_{22}H_{20}MoN_4O_5Re\cdot CH_2Cl_2$ (789.50): C 36.64, H 2.94, N 5.57; found: C 36.76, H 2.82, N, 5.33.

X-Ray Diffraction Analysis: Selected crystal and refinement data are given in Table 2. Diffraction data for **6** and **7** were collected on a Nonius Kappa-CCD diffractometer, using graphite-monochromated Mo-K α radiation. A semi-empirical absorption correction was performed with SORTAV.^[26] Diffraction data for **2**, **3** and **8–16** were collected on a Oxford Diffraction Xcalibur Nova single crystal diffractometer, using Cu-K α radiation. Empirical absorption corrections were applied using the SCALE3 ABSPACK algorithm as implemented in the program CrysAlis Pro RED (Oxford Diffraction Ltd., 2006).^[27] Structures were solved by Patterson interpretation using the program SIR2004.^[28] Isotropic and full matrix anisotropic least square refinements were carried out using SHELXL.^[29] H(5) hydrogen atom positions in **5** and **14** were located in the corresponding Fourier difference maps and were refined without restrictions. All the other hydrogen atoms were set in calculated positions and refined riding on their parent atoms. The molecular plots were made with the PLATON program package.^[30] The WINGX program system^[31] was used throughout the structure determinations. A se-

Table 2. Crystal data and refinement details for complexes **2**, **3**, **6**, **7**, **8**, **9**, **10**, **11**, **12**, **13**, **14**, **15**, **16**.

	2	3	6	7
empirical formula	$C_9H_{12}ClO_3ReS_3\cdot 3H_2O$	$C_{10}H_{15}O_6ReS_4\cdot H_2O$	$C_{53}H_{31}BF_{24}MoN_4O_2\cdot CH_2Cl_2$	$C_{54}H_{32}BF_{24}MoN_3O_2$
M_r	540.06	563.38	1403.49	1317.57
crystal system	Hexagonal	Triclinic	Monoclinic	Monoclinic
space group	$R\bar{3}$	$P1$	$C2/c$	$P21/c$
a [Å]	10.7117(2)	7.8568(3)	39.0390(4)	19.2279(2)
b [Å]	10.7117(2)	8.8845(4)	13.1465(1)	13.1162(2)
c [Å]	22.4874(2)	12.0286(4)	22.6607(2)	22.5679(4)
α [°]	90	94.615(3)	90	90
β [°]	90	100.239(3)	104.660(1)	111.555(5)
γ [°]	120	91.199(3)	90	90
V [Å 3]	2234.53(7)	823.06(6)	11251.44(17)	5293.52(14)
Z	6	2	8	4
T [K]	100(2)	100(2)	150(2)	293(2)
D_{calc} [g cm $^{-3}$]	2.381	2.274	1.657	1.875
$F(000)$	1560	544	55.840	2624
λ (K α) [Å]	1.5418	1.5418	0.71073	0.71073
crystal size [mm]	0.08 \times 0.11 \times 0.17	0.01 \times 0.03 \times 0.10	0.15 \times 0.17 \times 0.25	0.12 \times 0.15 \times 0.17
μ (K α) [mm $^{-1}$]	21.747	19.468	0.454	0.378
collection range [°]	5.16 to 66.18	3.75 to 73.77	1.82 to 25.36	1.82 to 25.34
max/min tran. factors	0.17/0.11	0.67/0.52	1.04/0.95	0.95/0.94
reflections collected	877	3251	10280	9577
indep reflect. $[R(int)]$	833[0.0550]	3173[0.0629]	9024[0.0662]	7496[0.0598]
goodness-of-fit on F^2	0.996	1.072	1.099	1.079
R , wR_2 (all data)	0.0332, 0.0768	0.0795, 0.2082	0.0825, 0.2149	0.0702, 0.1620
R , wR_2 ($I > 2\sigma(I)$)	0.0317, 0.0761	0.0788, 0.2068	0.0738, 0.2051	0.0506, 0.1340
	8	9	10	11
empirical formula	$C_{21}H_{19}ClMoN_4O_2$	$C_{21}H_{19}BrMoN_4O_2$	$C_{22}H_{22}MoN_4O_5S\cdot CH_2Cl_2$	$C_{44}H_{44}Mo_2N_8O_{10}S_2\cdot H_2O$
M_r	526.82	535.24	635.37	1118.91
crystal system	Monoclinic	Monoclinic	Monoclinic	Triclinic
space group	$C2/c$	$C2/c$	$P21/c$	$P\bar{1}$
a [Å]	27.234(2)	25.7655(3)	9.50590(1)	9.5059(4)
b [Å]	15.2912(7)	15.9479(2)	30.6741(4)	14.2386(4)
c [Å]	10.3759(4)	19.7950(2)	8.93270(1)	18.5203(6)
α [°]	90	90	90	99.920(3)
β [°]	92.163(7)	102.709(1)	98.9030(1)	96.675(4)
γ [°]	90	90	90	99.665(3)
V [Å 3]	4317.9(4)	7934.59(16)	2573.26(5)	2573.26(5)
Z	8	16	4	2
T [K]	100	100(2)	100(2)	100(2)
D_{calc} [g cm $^{-3}$]	1.621	1.792	1.640	1.625
$F(000)$	2128.0	4256.0	1288.0	1140.0

Table 2. (Continued)

	8	9	10	11
λ (K α) [Å]	1.5418	1.5418	1.5418	1.5418
crystal size [mm]	0.02 × 0.06 × 0.09	0.12 × 0.13 × 0.83	0.03 × 0.17 × 0.31	0.13 × 0.14 × 0.18
μ (K α) [mm ⁻¹]	6.357	7.985	7.204	5.934
collection range [°]	3.24 to 74.10	3.28 to 73.99	2.88 to 73.88	3.21 to 74.09
max/min tran. factors	0.74/0.69	0.70/0.10	0.80/0.26	0.47/0.43
reflections collected	4245	7883	5189	9044
indep reflect. [R(int)]	3296[0.0841]	6647[0.0262]	5057[0.0487]	8509[0.0829]
goodness-of-fit on F ²	0.987	1.000	1.008	1.017
R, wR ₂ (all data)	0.0906, 0.2054	0.0409, 0.1040	0.0445, 0.1416	0.0779, 0.2453
R, wR ₂ (<i>I</i> > 2 σ (<i>I</i>))	0.0726, 0.1842	0.0327, 0.0898	0.0416, 0.1228	0.0735, 0.2347
	12	13	14	15
empirical formula	C ₂₂ H ₂₀ ClMoN ₃ O ₂	C ₂₂ H ₂₀ BrMoN ₃ O ₂	C ₂₂ H ₂₀ IMoN ₃ O ₂	C ₂₂ H ₂₀ MoN ₄ O ₅
M _r	489.80	563.38	581.25	516.36
crystal system	Monoclinic	Monoclinic	Monoclinic	Monoclinic
space group	<i>P</i> 21/ <i>c</i>	<i>P</i> 21/ <i>c</i>	<i>P</i> 21/ <i>c</i>	<i>P</i> 21/ <i>c</i>
<i>a</i> [Å]	9.47600	19.3963(11)	19.9356(4)	19.5695(3)
<i>b</i> [Å]	13.2033	16.4011(10)	16.5037(5)	16.5757(2)
<i>c</i> [Å]	18.4396(1)	13.2390(7)	13.3274(3)	13.2932(2)
α [°]	90	90	90	90
β [°]	116.6300	100.345(5)	100.083(2)	100.7770(10)
γ [°]	90	90	90	90
<i>V</i> [Å ³]	5293.52(14)	4143.1(4)	4317.14(18)	4235.97(10)
<i>Z</i>	4	8	8	8
<i>T</i> [K]	100(2)	100(2)	100(2)	100(2)
<i>D</i> _{calc} [g cm ⁻³]	1.578	1.713	1.789	1.619
<i>F</i> (000)	992.0	2128.0	2272.0	2096.0
λ (K α) [Å]	1.5418	1.5418	1.5418	1.5418
Crystal size [mm]	0.03 × 0.05 × 0.08	0.01 × 0.02 × 0.03	0.03 × 0.10 × 0.15	0.02 × 0.05 × 0.07
μ (K α) [mm ⁻¹]	6.587	7.631	16.385	5.440
collection range [°]	4.29 to 73.99	3.55 to 74.10	3.50 to 75.20	3.35 to 73.95
max/min tran. factors	1.00/0.67	0.93/0.79	0.61/0.17	0.92/0.75
reflections collected	4174	8066	8659	8184
indep reflect. [R(int)]	3997[0.0224]	3218[0.1678]	8244[0.0520]	7240[0.0516]
goodness-of-fit on F ²	1.000	1.000	1.049	1.005
R, wR ₂ (all data)	0.0227, 0.0592	0.1938, 0.3378	0.0607, 0.1907	0.0441, 0.1111
R, wR ₂ (<i>I</i> > 2 σ (<i>I</i>))	0.0217, 0.0583	0.0946, 0.2661	0.0574, 0.1741	0.0392, 0.1069
	16			
empirical formula	C ₂₂ H ₂₀ MoN ₃ O ₆ Re·CH ₂ Cl ₂			
M _r	789.49			
crystal system	Monoclinic			
space group	<i>P</i> 21/ <i>c</i>			
<i>a</i> [Å]	11.2080(2)			
<i>b</i> [Å]	17.2669(3)			
<i>c</i> [Å]	13.3852(2)			
α [°]	90			
β [°]	101.834(2)			
γ [°]	90			
<i>V</i> [Å ³]	2535.35(7)			
<i>Z</i>	4			
<i>T</i> [K]	100			
<i>D</i> _{calc} [g cm ⁻³]	2.068			
<i>F</i> (000)	1520.0			
λ (K α) [Å]	1.5418			
crystal size [mm]	0.02 × 0.04 × 0.09			
μ (K α) [mm ⁻¹]	15.573			
collection range [°]	3.35 to 73.72			
max/min tran. factors	0.70/0.48			
reflections collected	4904			
indep reflect. [R(int)]	4162[0.0427]			
goodness-of-fit on F ²	1.001			
R, wR ₂ (all data)	0.0567, 0.1387			
R, wR ₂ (<i>I</i> > 2 σ (<i>I</i>))	0.0461, 0.1309			

lection of crystal, measurement, and refinement data is given in Table 2. Despite many attempts, only low quality crystals of **5** could be achieved. The poor diffraction data set obtained from one of these crystals accounted for persistent NPD thermal ellipsoids after refinement. However, the atomic connectivity in **5** could be inferred from these data, as shown in Figure 4. This material is available from the authors as supplementary material. CCDC-956351 (2), 956352 (3), 956353 (6), 956354 (7), 956355 (8), 956356 (9), 956357 (10), 956358 (11), 956359 (12), 956360 (13), 956361 (14), 956362 (15), and 956363 (16) contain the supplementary crystallographic data for this paper. These data can be obtained free of charge from The Cambridge Crystallographic Data Centre via www.ccdc.cam.ac.uk/data_request/cif.

Acknowledgements

We thank Principado de Asturias (Grant IB08–104 administered by FICYT), FEDER funds, and Ministerio de Economía y Competitividad (CTQ2012–37379-C02–01).

Keywords: host–guest systems · hydrogen bonds · metal complexes · receptors · tris(2-pyridyl) · trithiacyclononane

- [1] K. Bowman-James, A. Bianchi, E. García-España, *Anion Coordination Chemistry*, Wiley-VCH, Weinheim, **2011**; V. Amendola, L. Fabbrizzi, L. Mosca, *Chem. Soc. Rev.* **2010**, *39*, 3889–3915; J. L. Sessler, P. Gale, W.-S. Cho, in *Anion Coordination Chemistry* (Ed.: J. F. Stoddart), RSC, Cambridge, **2006**; P. A. Gale, *Acc. Chem. Res.* **2006**, *39*, 465–475; V. Amendola, D. Esteban-Gómez, L. Fabbrizzi, M. Licchelli, *Acc. Chem. Res.* **2006**, *39*, 343–353; F. P. Schmidtchen, *Top. Curr. Chem.* **2005**, *255*, 1–29; K. Choi, A. D. Hamilton, *Coord. Chem. Rev.* **2003**, *240*, 101–110; J. W. Steed, J. L. Atwood, *Supramolecular Chemistry*, Wiley, Chichester, **2000**; A. Bianchi, K. Bowman-James, E. García-España, *Supramolecular Chemistry of Anions*, Wiley-VCH, New York, **1997**; F. P. Schmidtchen, M. Berger, *Chem. Rev.* **1997**, *97*, 1609–1646; J. M. Lenn, *Supramolecular Chemistry*, 1st ed., Wiley-VCH, Weinheim, **1995**.
- [2] J. Pérez, L. Riera, *Chem. Commun.* **2008**, 533–543; J. Pérez, L. Riera, *Chem. Soc. Rev.* **2008**, *37*, 2658–2667; C. R. Rice, *Coord. Chem. Rev.* **2006**, *250*, 3190–3199; M. H. Filby, J. W. Steed, *Coord. Chem. Rev.* **2006**, *250*, 3200–3218; P. D. Beer, E. J. Hayes, *Coord. Chem. Rev.* **2003**, *240*, 167–189; P. D. Beer, P. A. Gale, *Angew. Chem.* **2001**, *113*, 502–532; *Angew. Chem. Int. Ed.* **2001**, *40*, 486–516; M. G. Fisher, P. A. Gale, M. E. Light, S. J. Loeb, *Chem. Commun.* **2008**, 5695–5697; I. D. Vega, P. A. Gale, M. E. Light, S. J. Loeb, *Chem. Commun.* **2005**, 4913–4915; C. R. Bondy, P. A. Gale, S. J. Loeb, *J. Am. Chem. Soc.* **2004**, *126*, 5030–5031; C. R. Bondy, P. A. Gale, S. J. Loeb, *Chem. Commun.* **2001**, 729–730.
- [3] L. Ion, D. Morales, S. Nieto, J. Pérez, L. Riera, V. Riera, D. Miguel, R. A. Kowenicki, M. McPartlin, *Inorg. Chem.* **2007**, *46*, 2846–2853; P. D. Beer, S. W. Dent, G. S. Hobbs, T. J. Wear, *Chem. Commun.* **1997**, 99–100. For an example of a non metal-based anion host that employs a combination of N-H and C–H bonds to bind anions, see: C. A. Ilioudis, D. A. Tocher, J. W. Steed, *J. Am. Chem. Soc.* **2004**, *126*, 12395–12402. For an example of a non metal-based anion host that employs exclusively C–H groups for anion binding, see: Y. Hua, R. O. Ramabhadran, E. O. Udehji, J. A. Karty, K. Raghavachari, A. H. Flood, *Chem. Eur. J.* **2001**, *17*, 312–321.
- [4] R. D. Bedford, M. Betham, C. P. Butts, S. J. Coles, M. B. Hursthouse, P. N. Scully, J. H. R. Tucker, J. Wilkie, Y. Willener, *Chem. Commun.* **2008**, 2429–2431.
- [5] P. K. Baker, S. J. Coles, M. C. Durrant, S. D. Harris, D. L. Hughes, M. B. Hursthouse, R. L. Richards, *J. Chem. Soc. Dalton Trans.* **1996**, 4003–4010; D. L. Lichtenberger, *Inorg. Chem.* **1985**, *24*, 636–638; R. S. Glass, G. S. Wilson, W. N. Setzer, *J. Am. Chem. Soc.* **1980**, *102*, 5068–069.
- [6] D. Morales, M. Puerto, I. del Río, J. Pérez, R. López, *Chem. Eur. J.* **2012**, *18*, 16186–16195.
- [7] S. Nieto, J. Pérez, L. Riera, V. Riera, D. Miguel, J. A. Golen, A. L. Rheingold, *Inorg. Chem.* **2007**, *46*, 3407–3418.
- [8] C. Pomp, S. Druéeke, H. J. Kueppers, K. Wiegardt, C. Krueger, B. Nuber, J. Weiss, *Z. NATURFORSCH B* **1988**, *43*, 299–305.
- [9] L. F. Szczepura, L. M. Witham, K. J. Takeuchi, *Coord. Chem. Rev.* **1998**, *174*, 5–32.
- [10] A. Maleckis, J. W. Kampf, M. S. Sanford, *J. Am. Chem. Soc.* **2013**, *135*, 6618–6625.12.
- [11] G. E. Schneider, H. J. Bolink, E. C. Constable, C. D. Ertl, C. E. Housecroft, A. Pertegàs, J. A. Zampese, A. Kanitz, F. Kessler, S. B. Meie, *Dalton Trans.* **2013**, DOI: 10.1039/c3dt53229.
- [12] W. M. Ward, B. H. Farnum, M. Siegler, G. J. Meyer, *J. Phys. Chem. A* **2013**, *117*, 8883–8894.
- [13] M. Brookhart, B. Grant, A. F. Volpe Jr., *Organometallics* **1992**, *11*, 3920–3922.
- [14] M. Pietrzak, J. P. Wehling, S. Kong, P. M. Tolstoy, I. G. Shenderovich, C. López, R. M. Claramunt, J. Elguero, G. S. Denisov, H.-H. Limbach, *Chem. Eur. J.* **2010**, *16*, 1679–1690.
- [15] H. Martínez-García, D. Morales, J. Pérez, M. Puerto, D. Miguel, *Inorg. Chem.* **2010**, *49*, 6974–6985.
- [16] T. Perera, P. A. Marzilli, F. R. Fronczek, L. G. Marzilli, *Inorg. Chem.* **2010**, *49*, 5560–5572.
- [17] M. J. Hynes, *J. Chem. Soc. Dalton Trans.* **1993**, 311–312.
- [18] H. T. Dieck, H. Friedel, *J. Organomet. Chem.* **1968**, *14*, 375–385.
- [19] H. Elias, G. Schmidt, H.-J. Küppers, M. Saher, K. Wiegardt, B. Nuber, J. Weiss, *Inorg. Chem.* **1989**, *28*, 3021–3024.
- [20] R. Bieda, M. Dobrosckke, A. Triller, I. Ott, M. Spehr, R. Gust, A. Prokop, W. S. Sheldrick, *ChemMedChem* **2010**, *5*, 1123–1133.
- [21] A. J. Blake, A. J. Holder, T. I. Hyde, H. J. Küppers, M. Schröder, S. Stötzel, K. Wiegardt, *J. Chem. Soc. Chem. Commun.* **1989**, 1600–1602.
- [22] M. A. Bennett, L. Y. Goh, A. C. Willis, *J. Am. Chem. Soc.* **1996**, *118*, 4984–4992.
- [23] W. Yang, H. Schmider, Q. Wu, Y.-s. Zhang, S. Wang, *Inorg. Chem.* **2000**, *39*, 2397–2404.
- [24] See, for instance: a) P. A. Anderson, F. R. Keene, E. Horn, E. R. T. Tiekink, *Appl. Organomet. Chem.* **1990**, *4*, 523–533; b) N. M. Shavaleev, A. barbieri, Z. R. Bell, M. D. Ward, F. Barigelleti, *New J. Chem.* **2004**, *28*, 398–405.
- [25] K. J. Reimer, A. Shaver, *Inorg. Synth.* **1990**, *28*, 154–159.
- [26] R. H. Blessing, *Acta Crystallogr.* **1995**, *A51*, 33–38.
- [27] *CrysAlisPro RED*, version 1.171.31.7; Oxford Diffraction Ltd.: Oxford, UK, **2009**.
- [28] M. C. Burla, R. Caliandro, M. Camalli, B. Carrozzini, G. L. Cascarano, L. De Caro, C. Giacovazzo, G. Polidori, R. Spagna, *J. Appl. Cryst.* **2005**, *38*, 381–388.
- [29] Sheldrick, G. M. *SHELXL*, version 2008. *Acta Crystallogr.* **2008**, *A64*, 112.
- [30] A. L. Spek, A. L. *PLATON* version 1.15: A Multipurpose Crystallographic Tool; University of Utrecht: Utrecht, The Netherlands, **2008**.
- [31] L. J. Farrugia, *J. Appl. Crystallogr.* **1999**, *32*, 837–838.

Received: September 16, 2013

Revised: January 5, 2014

Published online on March 27, 2014